Proprietes (statistiques) des galaxies

J. Devriendt, CRAL

Plan

- Le contexte historique
- Types de galaxies et proprietes physiques/relations fondamentales
- Statistique des proprietes des galaxies locales (SDSS) sauf clustering
- Statistique des proprietes des galaxies lointaines (LBGs) sauf clustering

I- Introduction historique

Around 1610:
Galilei resolves the Milky Way into many faint stars (discovery due to introduction of telescopes; other discoveries: Jupiter moons, sun spots).
Around 1750:
Building on a popular summary of Thomas Wright's first (bizarre) ideas about the structure of the Milky Way, Immanuel Kant concludes that the appearance of the Milky Way is best explained by a disk of stars. Furthermore he claims that the faint elliptical nebulae observed by de Maupertuis are very distant 'island universes' resembling in shape and composition our own Milky Way.
Late 18th century:
Herschel uses systematic star counts to determine the flattening of the Milky Way and obtains 1:5. He compiles a list of nebulae and discriminates between nebulaewith embedded stars (like the Orion nebula) and others which appear to be 'a shining fluid of a nature totally unknown to us'.

Middle of 19th century:
William Parsons discovers spiral structures in some nebulae and concludes that they rotate.
Late 19th century:
Photographic plates revolutionize astronomical observations. Kapteyn, von Seeliger and van Rijn discuss the structure of the Milky Way in a new quantitative way based on reliable star counts on plates. Kapteyn concludes that the Milky Way has a radius of a few kiloparsecs and that the sun is at its center. At the same time Shapley reasons that the sun is located at 15kpc distance from the center because of the distribution of globular clusters in the sky. (This contradiction is later resolved by the discovery of interstellar extinction.)
1923/24:
With the new 100 inch telescope on Mount Wilson (and building on previous results), Edwin Hubble uncovers the true nature of the ’nebulae’. He resolves M31and M33 into faint stars, and confirms that these systems are galaxies like the Milky Way. He identifies Cepheids in these objects and determines their distance (then: 300kpc, modern value: 770kpc).

1926/27:
B.Lindblad and J.Oort derive the first realistic model of the Galaxy. They determine its rotation velocity to 200 km/s to 300 km/s (modern value 220 km/s) and estimate its mass.
1929:
Hubble discovers the expansion of the Universe and determines the Hubble constant to 530 km/s/Mpc (today: 70 km/s/Mpc).
1930:
Trumpler demonstrates the existence of an absorbing interstellar material.
Thirties:
Fritz Zwicky observes the redshifts of individual galaxies in the Coma cluster and finds first evidence for ‘dark matter’. (Nobody believes him...)
1944:
During the wartime blackout of Los Angeles, Walter Baade discovers the differences in the stellar populations between the center of M31, its companions and the solar neighborhood (Population I and II, i.e. young and old).

1944:
van der Hulst predicts the HI-Emission of neutral atomic hydrogen (hyperfine structure transition at 21cm wavelength). This emission is discovered in 1951 using the newly developed radar technology.
1962:
Maarten Schmidt discovers Quasars as first objects of significant redshift.
1965:
Penzias and Wilson discover the 3K microwave background (as predicted by Gamov et al. in 1940).
Seventies:
Evidence for dark matter becomes stronger, mostly due to flat rotation curves of spiral galaxies. (This leads to the standard cold-dark-matter model of the eighties).
Eighties:
Second revolution in astronomical observing techniques: In the optical wavelength region, Charge Coupled Devices (CCDs) improve the detection sensitivities by a factor 10 to 100 relative to photographic plates. Satellites provide new observing windows in the infrared and X-rays. It is now possible to study the structure, dynamics, stellar populations and interstellar medium of external galaxies in detail.The systematic study of the large-scale-structure of the Universe begins.

Nineties:
A quantum jump in spatial resolution is provided by the Hubble-Space-Telescope. 10m class telescopes are being built. Both lead to a boom in extragalactic studies and cosmology. Fluctuations in the cosmic microwave background are detected at a level of 10^{-5}. Galaxies and Quasars are now found at redshifts of 5 and beyond.
21st century:
Large scale surveys of local galaxy (2dF, SDSS) are completed containing several hundred of thousand galaxies, opening a new era for statistical analysis.

II- Types de galaxies et proprietes fondamentales

Galaxy Classification Schemes

Classification schemes usually based on a restricted and incomplete set of information (e.g. morphology in blue-band photography).
Classical classifications schemes have biases of various sorts: optical bias, surface brightness bias, luminosity bias.
Classification not always well-defined or unique.
Nevertheless morphological classification is useful: the isolation of some fundamental properties of galaxies provides guidance to pose questions that result in quantitative analysis and better physical understanding of the objects.

Examples of classification schemes:
Hubble-Sandage (1936)
de Vaucouleurs (1959)
van den Bergh (1960/66)
Yerkes (Morgan, 1957)
...
Primary classification criteria of commonly used Hubble-Sandage system:
Disk-to-bulge ratio
Opening angle of spiral arms
Bars

System Principal criteria Symbols Examples
Hubble-Sandage barrishness; E, S0, S, SB, Irr M87=E1
(Sandage openness of arms/disk-bulge ratio; a, b, c M31=Sb
(1961-1995)) degree of resolution of arms into stars M101=Sc
LMC=Irr I
De Vaucouleurs barrishness; E, S0, S, SA, SB, I M87=E1P
(de Vaucouleurs openness of arms/disk-bulge ratio; a, b, c, d, m
M31=SA(s)b (1959)) rings or s shapes (r), (s) M101=SAB(rs)cd
LMC=SB(s)c
Yerkes central concentration of light; k, g, f, a M87=kE1
(Morgan barishness/smoothness E, R, D, S, B, I M31=kS5
(1958-1970)) M101=fS1, LMC= afI2
DDO richness of disk in young stars; E, S0, A, S, Ir M87=E1
(van den Bergh barrishness; B M31=Sb I-II
(1960-1976)) central concentration of light; a, b, c M101=Sc I
quality and length of arms I, II,. . . , V LMC=Ir III-IV

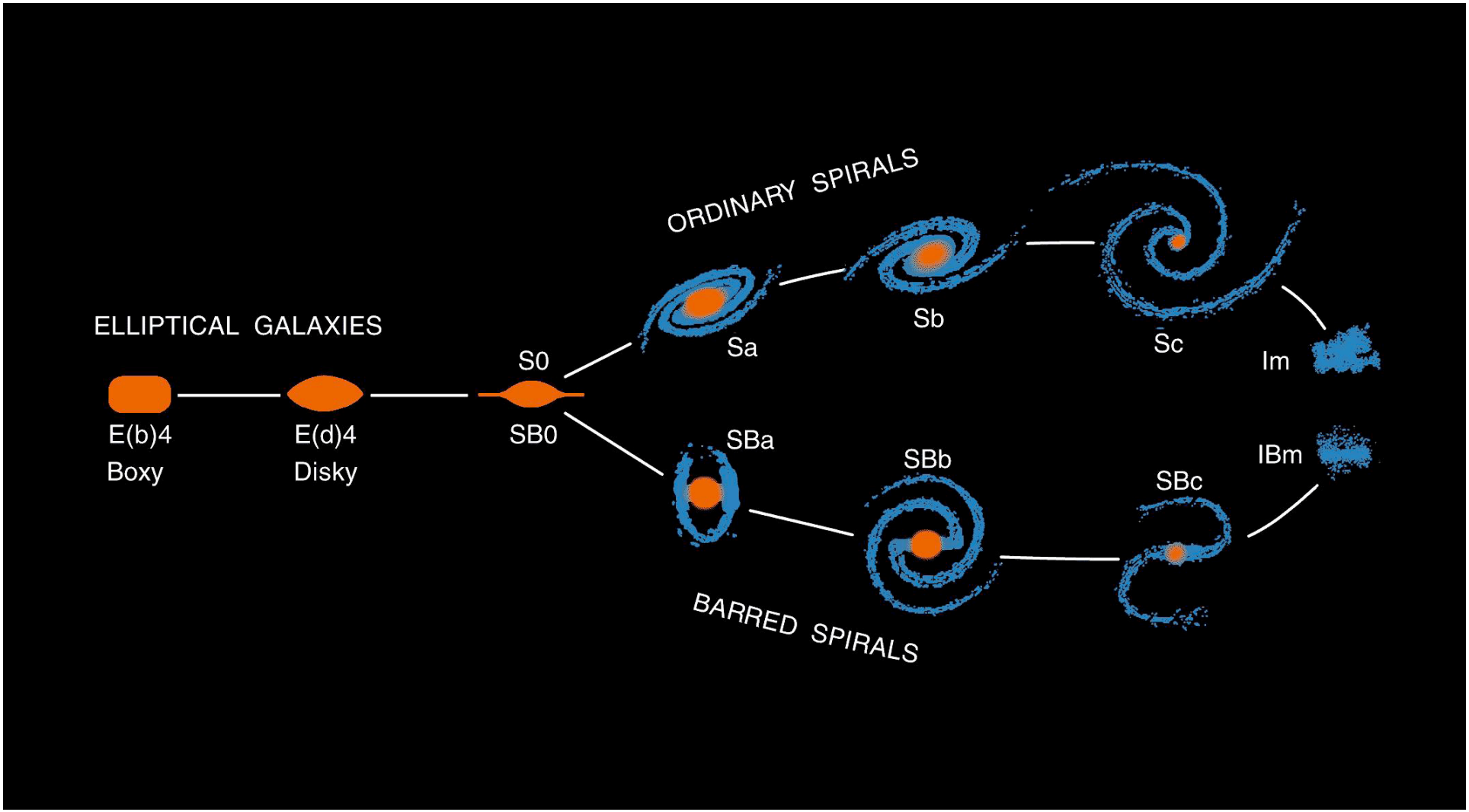
ELLIPTICAL GALAXIES
E(b)4
Boxy
E(d)4
Disky
S0
SB0
ORDINARY SPIRALS
Sa
Sb
Sc
Im
SBa
SBb
SBc
IBm
BARRED SPIRALS

Elliptical (E) Galaxies:

M 87: E0-galaxy

M 110: E6-galaxy

Lenticular (S0) Galaxies:

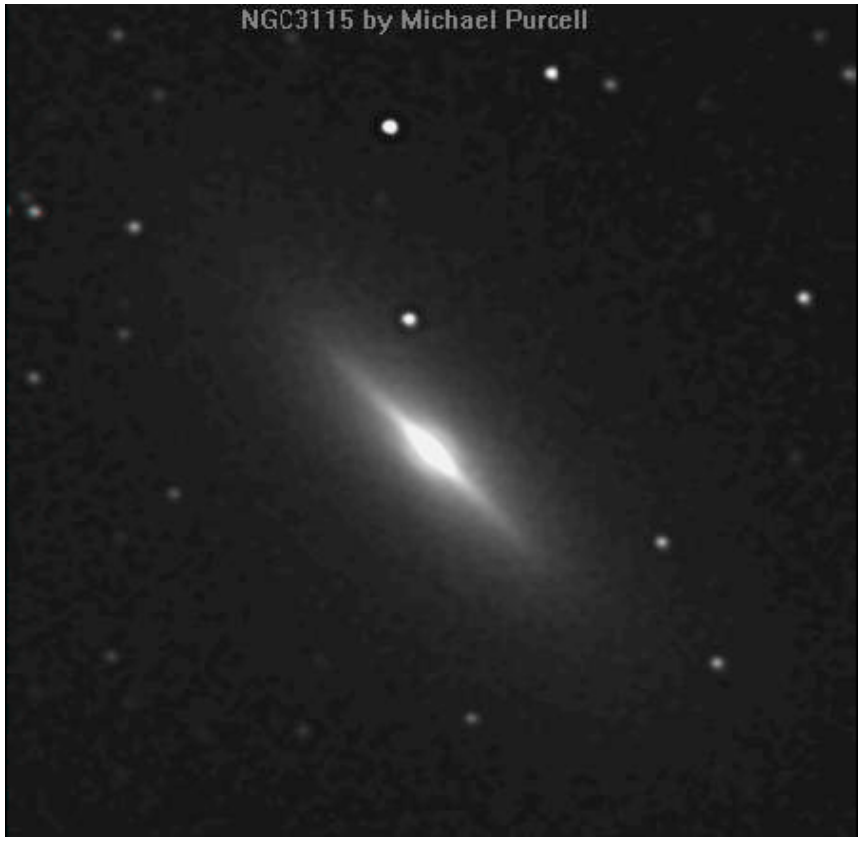

NGC 3115: S0-galaxy

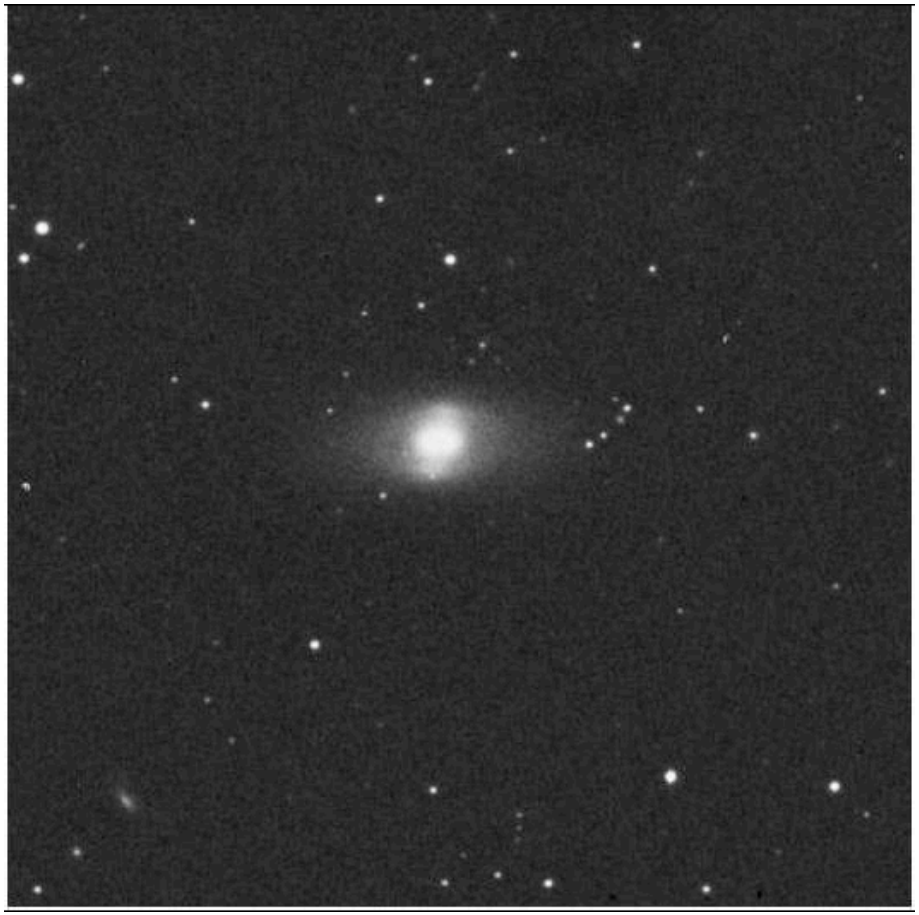

NGC 4371: SB0-galaxy

Spiral (Sa) Galaxies:

NGC 3223: Sa-galaxy

M 104 (Sombrero), Sa-galaxy

Spiral (Sb) Galaxies:

M 31 (Andromeda-galaxy):
Sb-galaxy

M 81: Sb-galaxy

Spiral (Sc) Galaxies:

M 51: Sc-galaxy

M 101: Sc-galaxy

Barred-Spiral (SBa) Galaxies:

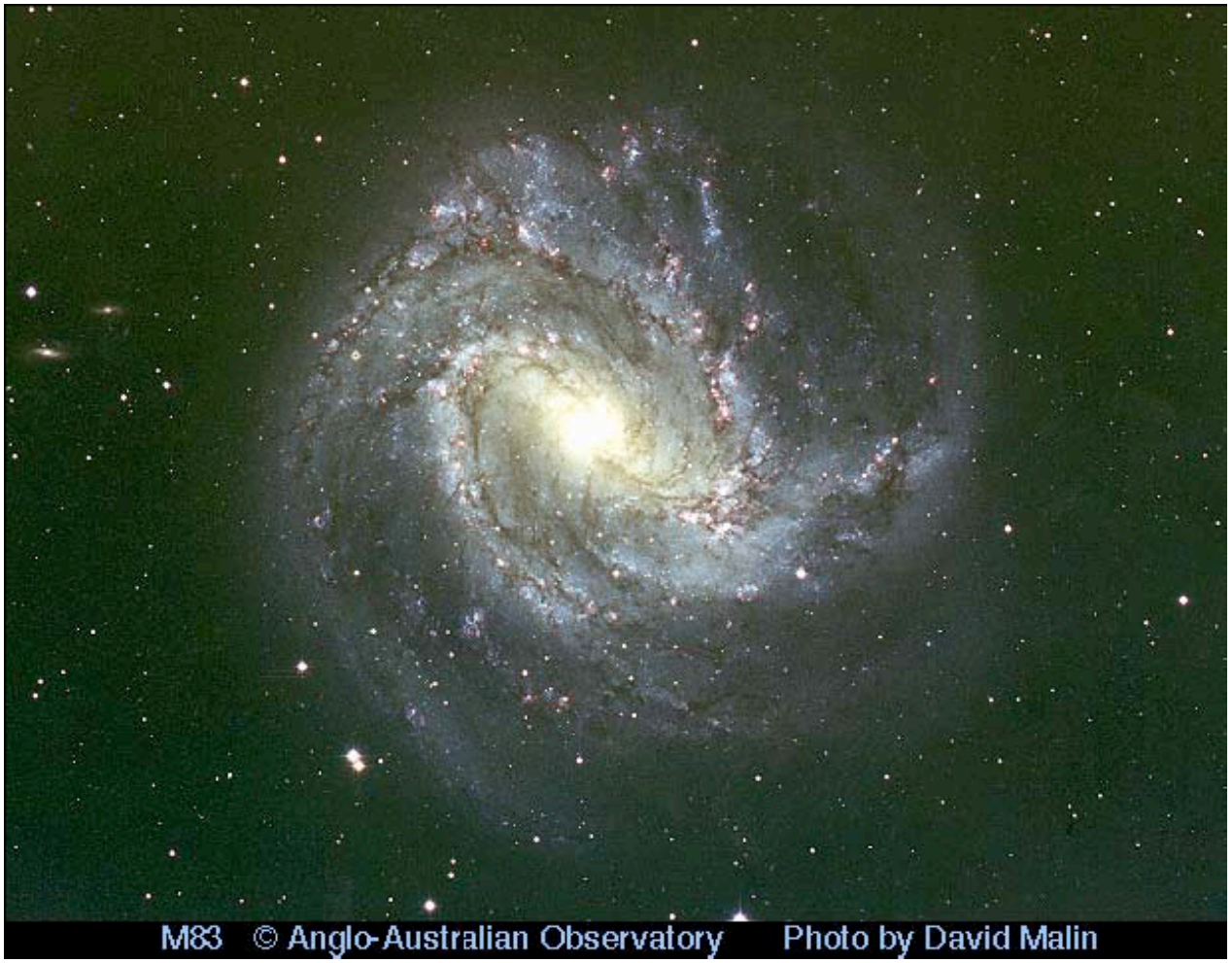

M 83 (Southern Pinwheel):
SBa-galaxy

Barred-Spiral (SBb) Galaxies:

M 95: SBb-galaxy

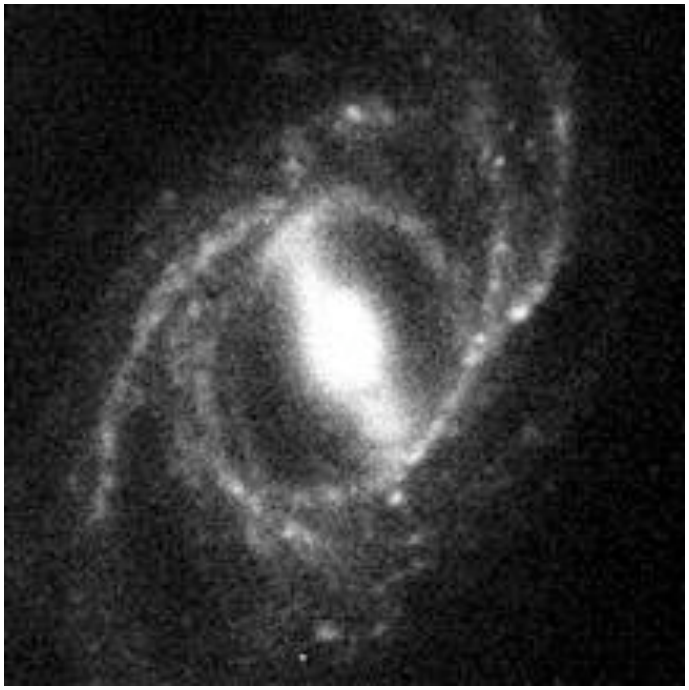

NGC 2523: SBb-galaxy

Barred-Spiral (SBc) Galaxies:

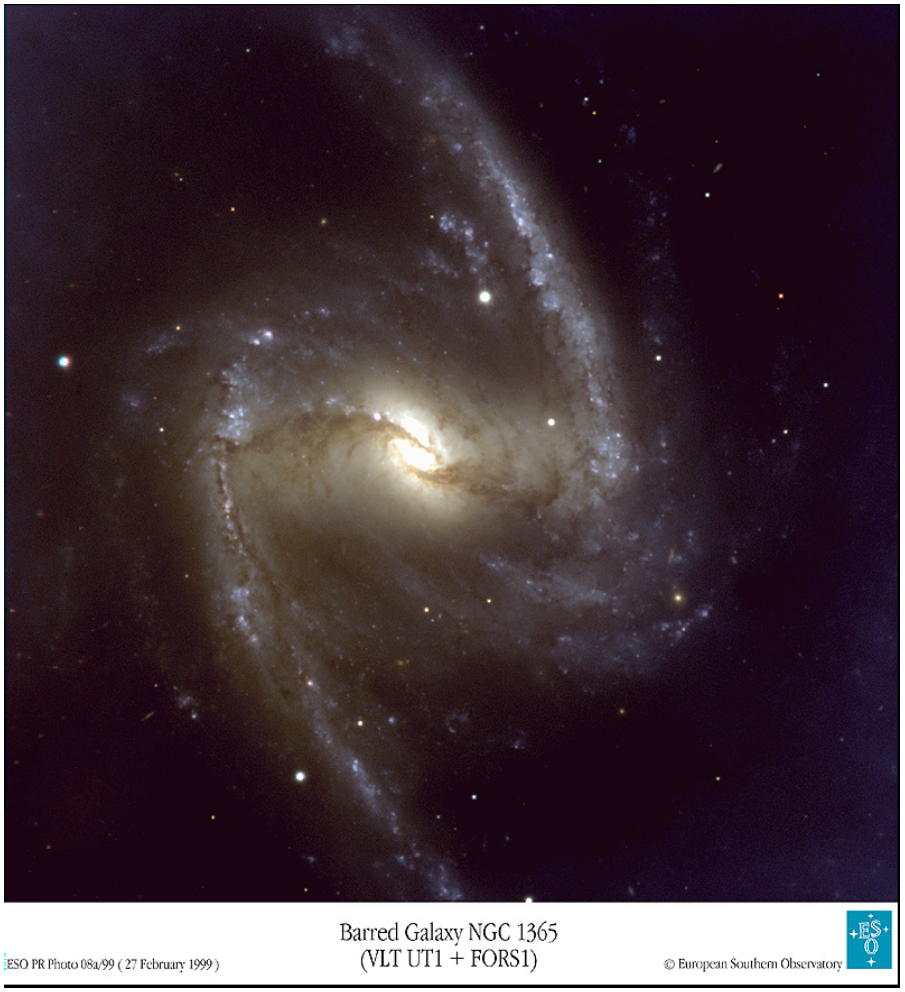

NGC 1365: SBc-galaxy

NGC 613: SBc-galaxy

Irregular (Irr) Galaxies:

LMC: Irr-galaxy

SMC: Irr-galaxy

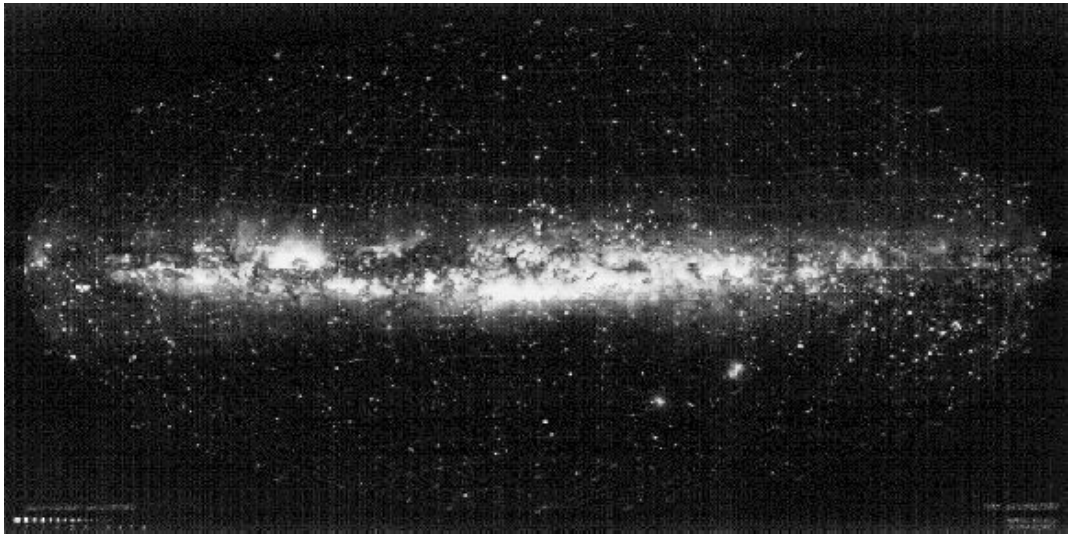

Milky Way, Sbc-galaxy (all-sky projection in optical)

Milky Way, Sbc-galaxy (all-sky projection in near IR, COBE satellite)

Other Galaxy Types

Classical classification systems are incomplete regarding:
=> dwarf galaxies:
dE: dwarf ellipticals or dwarf spheroidals, similar to E but low luminosity and low surface brightness
BCD: Blue Compact Dwarfs, concentrated starburst, few old stars some extreme types:
=> cD-galaxies: Yerkes classification for “extra (c) large and diffuse (D)” galaxies, found in the centers of clusters and groups
=> low surface brightness (LSB) galaxies: luminous but very low surface brightness disks
=> active galaxies: radio galaxies; galaxies with unusual nuclear emission lines and/or extreme nuclear luminosity (QuasiStellarObjects-QSOs, Seyfert galaxies) and/or with powerful non-thermal radio emission (radio galaxies, quasars)
=> interacting, merging and starbursting galaxies

Dwarf Galaxies:

Leo 1, dwarf elliptical (dwarf spheroidal) companion of Milky Way

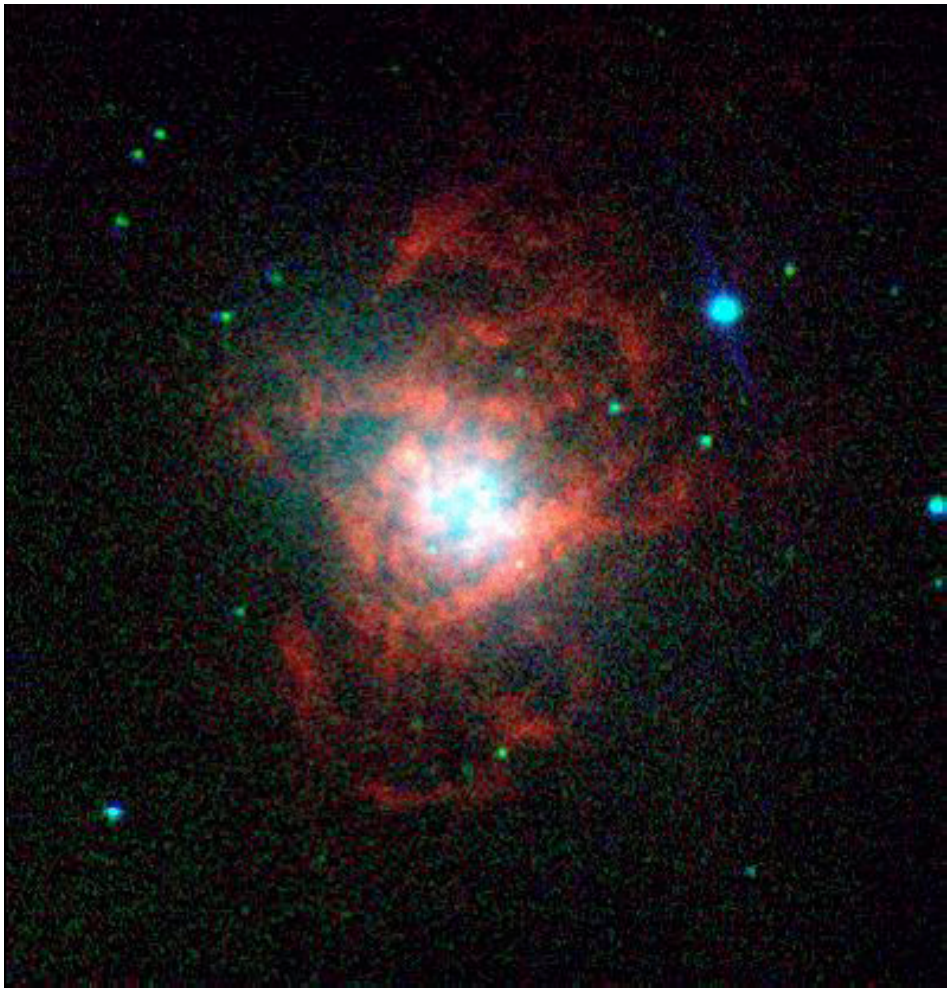

Blue Compact Dwarf (BCD) NGC 1705, blue: blue continuum, green: red continuum, red: H

Active Galaxies:

NGC 7742, a Seyfert galaxy

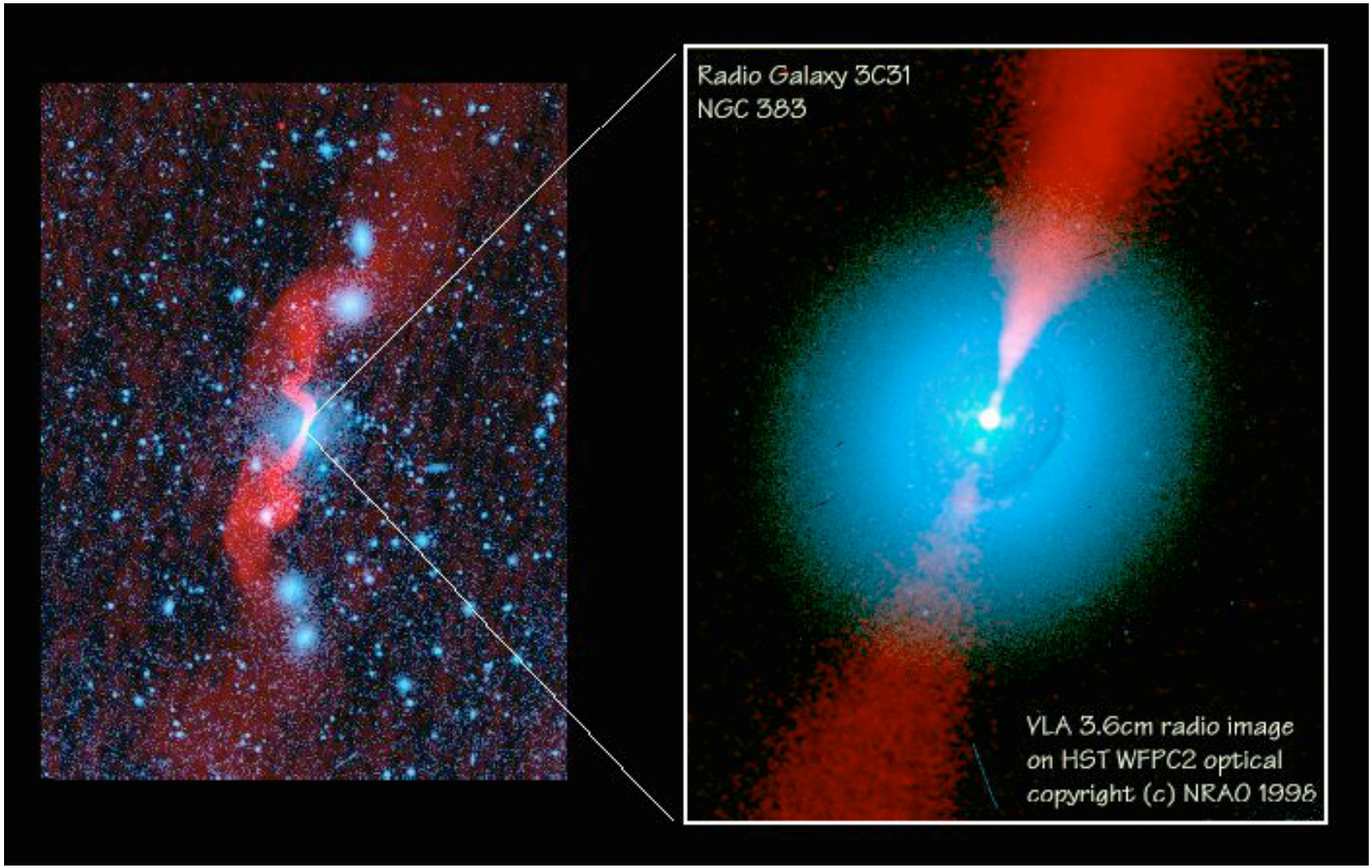

NGC 383 (= 3C31), a radio galaxy, blue: optical, red: radio

Interacting, Merging and Starbursting Galaxies:

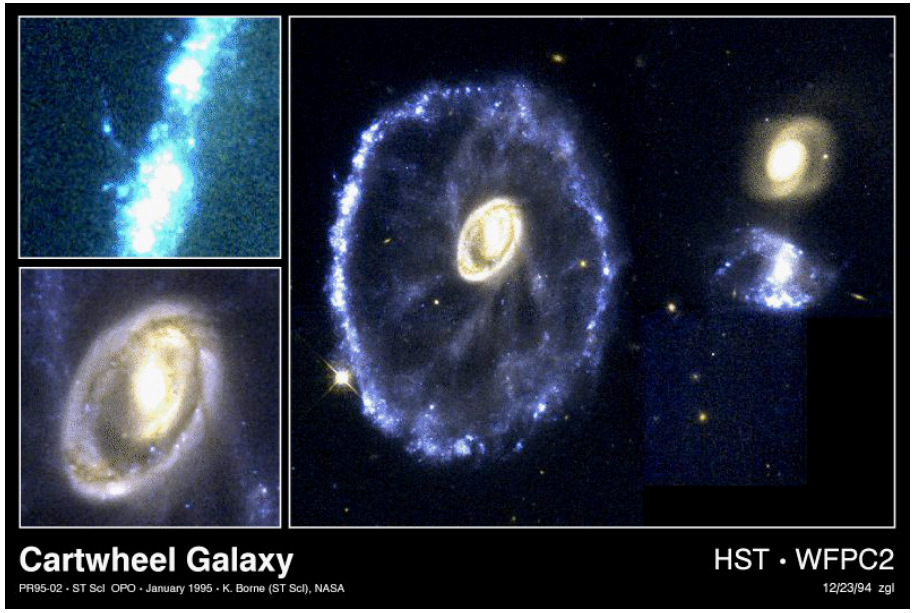

Cartwheel galaxy

Antenna galaxies

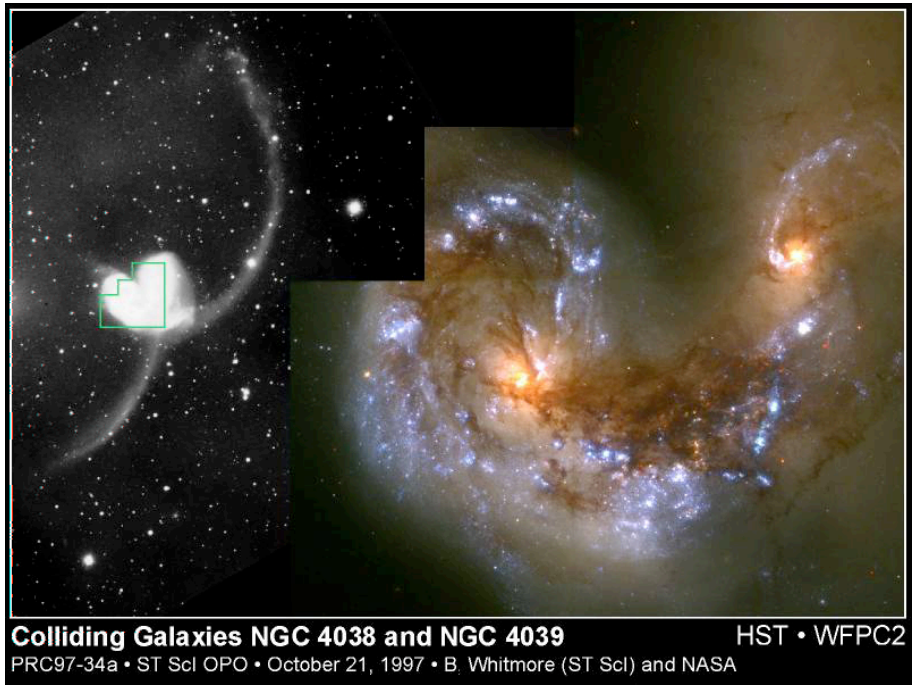

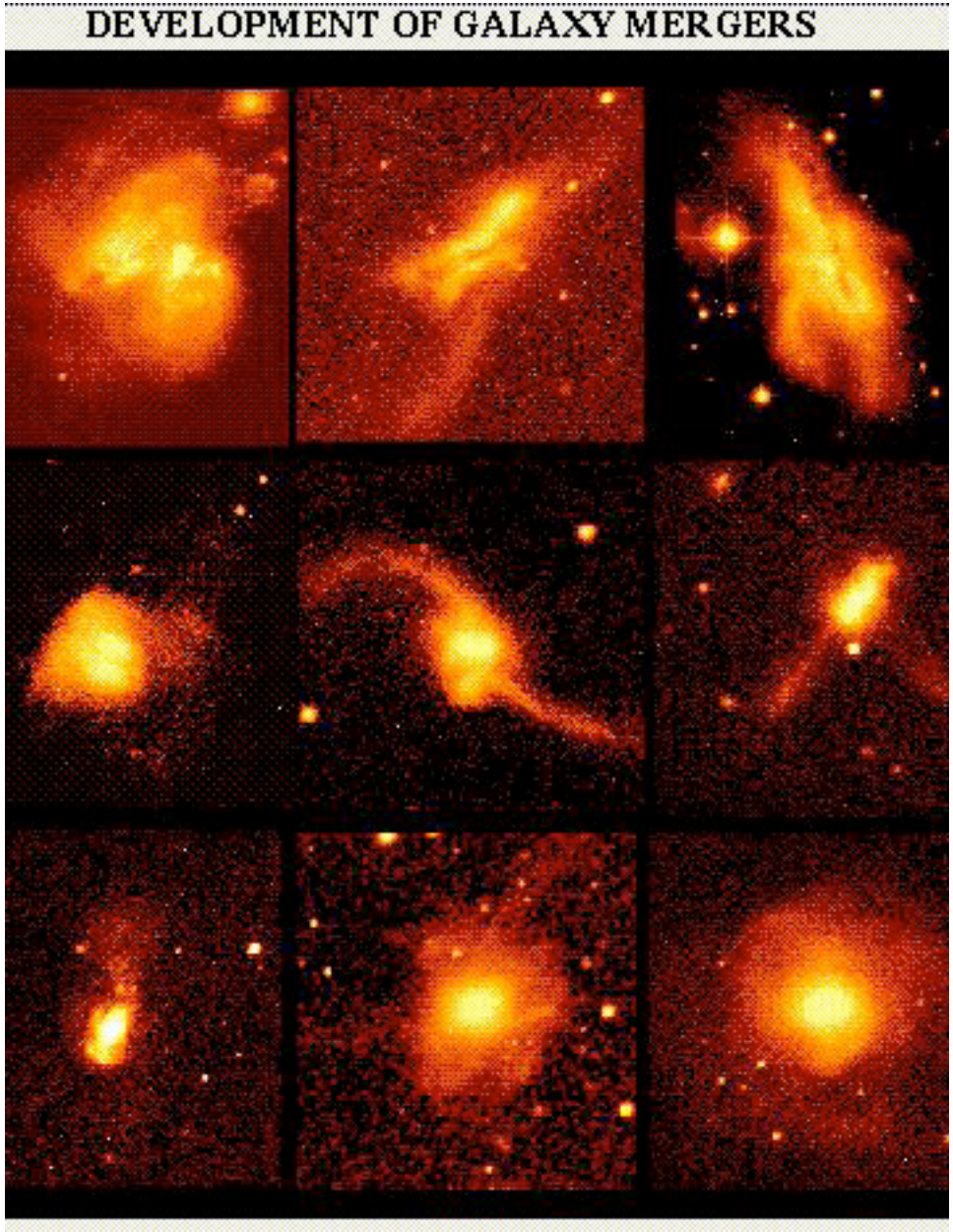

Various evolutionary steps of spiral-spiral mergers

Galaxies at Non-optical Wavelengths:

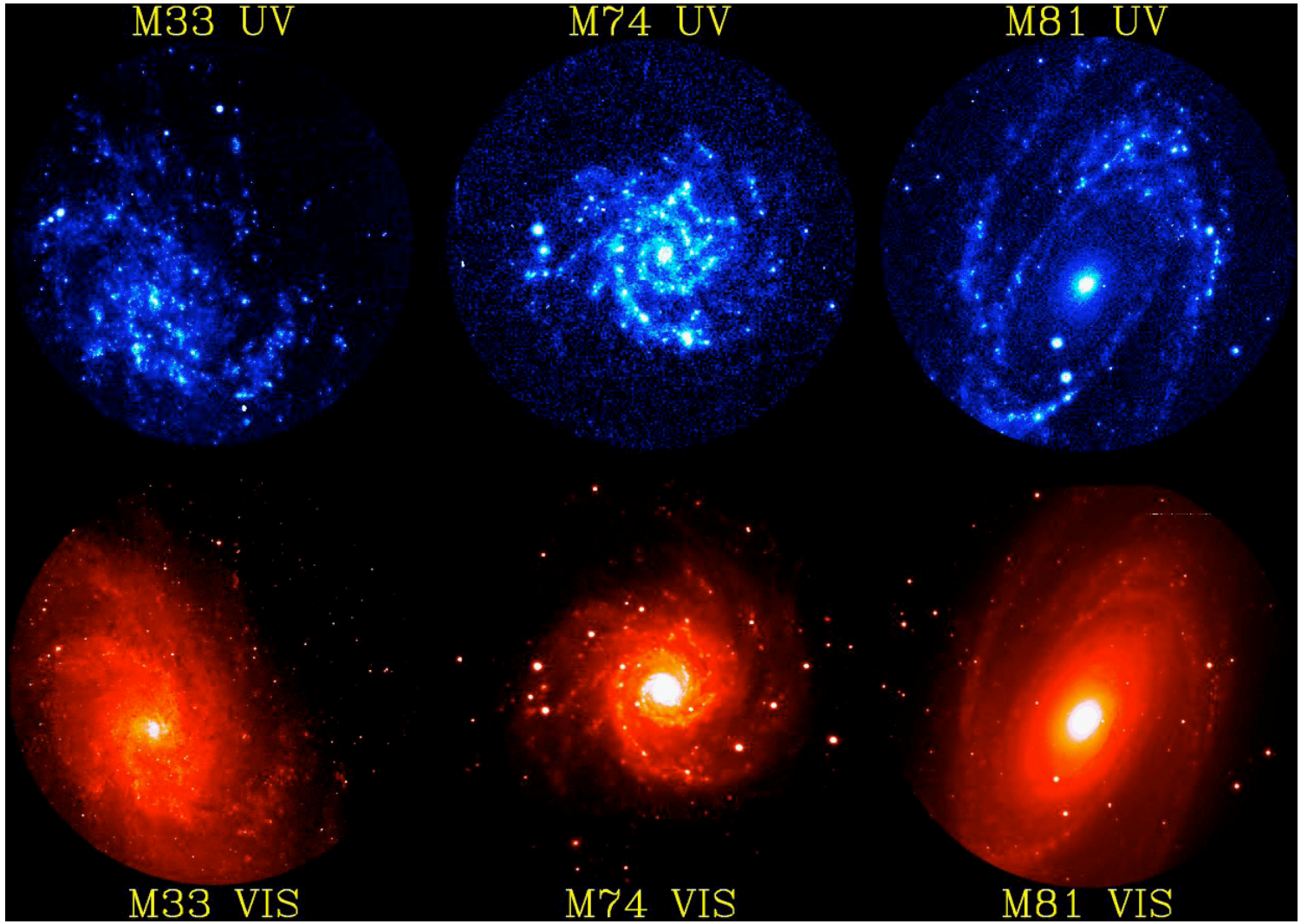

Spirals in ultraviolet (dominated by massive stars) and visual (average population)

Multiwavelength Milky Way

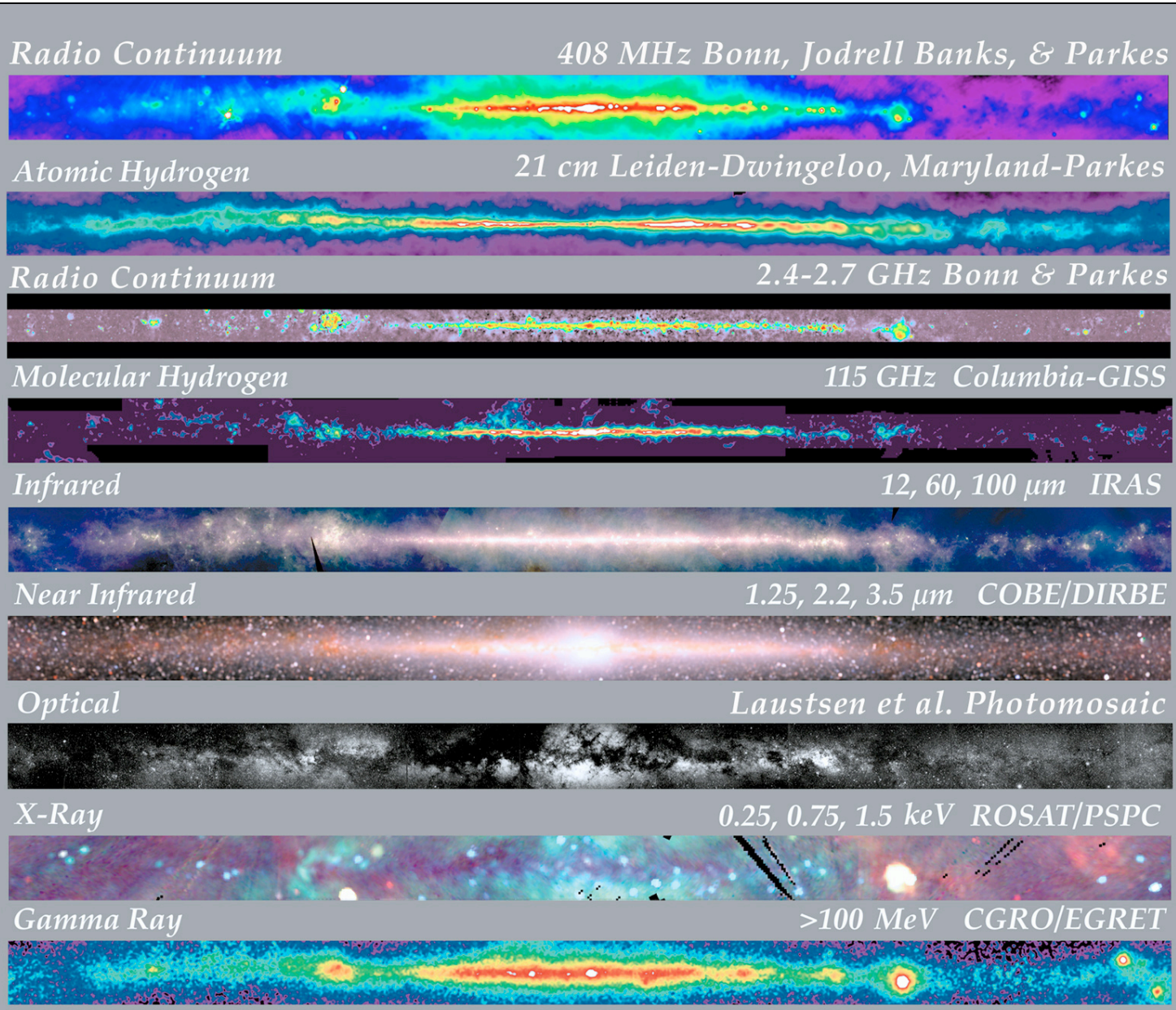

NASA

ASTROPHYSICS DATA FACILITY
ADF
GODDARD SPACE FLIGHT CENTER

Mass-Luminosity Ratios

Usually with reference to the luminosity in B (L_B) or the visual luminosity (L_V) and normalized to the sun.
sun :M/L= 1 M_{sun} /L_{Bsun};
stars : log L /L_{sun} approx 3.8 log M/M_{sun}
star with mass M = 0.5 M_{sun} --> M/L = 10 M_{sun} / L_{sun}
star with mass M = 2M_{sun} --> M/L = 0.1 M_{sun} / L_{sun}

In star systems the luminosity is dominated by massive stars, the mass by low-mass stars (due to their longer lifetime and greater number).

Luminous parts of « normal » galaxies have M/L approx 10 M_{sun}/L_{Bsun} (metallicity dependent) valid also for solar neighborhood

Luminosity Function of Schechter
see: Schechter P. (1976) ApJ, 203, 297

global fitting function for all galaxies
(individual types do not follow the Schechter-function)
$\Phi(L/L_{star}) = \Phi_{star} \times (L/L_{star})^{alpha} \times \exp -L/L_{star}$

typical values (averaged over large volumes)
$L_{star} = 10^{10} L_{Bsun} h^{-2}$
or: $M_{Bsun} = -19.5 + 5 \log h$
$\Phi_{star} = 0.01 Mpc^{-3} h^{3}$
alpha = -1 … -1.3 (see Peebles 1993)

Cut off at low luminosity --> not yet observed

with: $h = H_0 / 100\text{km/s/Mpc}$
and $M_B = -2.5 \log L/L_{Bsun} + 5.48$

Phi (L/L_{star}) dL is the number density of galaxies with luminosities in the range (L; L + dL)
(strong variation of depending on environment)

averaged luminosity per volume:
$j = \text{int}\,[0,\text{inf}]\; L\, \text{Phi}(L/L_{star})\, dL/L_{star}$
$L = \text{Gamma}(\text{alpha} + 2)\; \text{Phi}_{star}\, L_{star}$
--> $j = 10^8\, L_{sun} / \text{Mpc}^3$
Using M / L = 10 yields a mass density of
$\text{Rho}_{star} = 10^9\, M_{sun} / \text{Mpc}^3$
$\text{Omega}_{star} = 0.004$

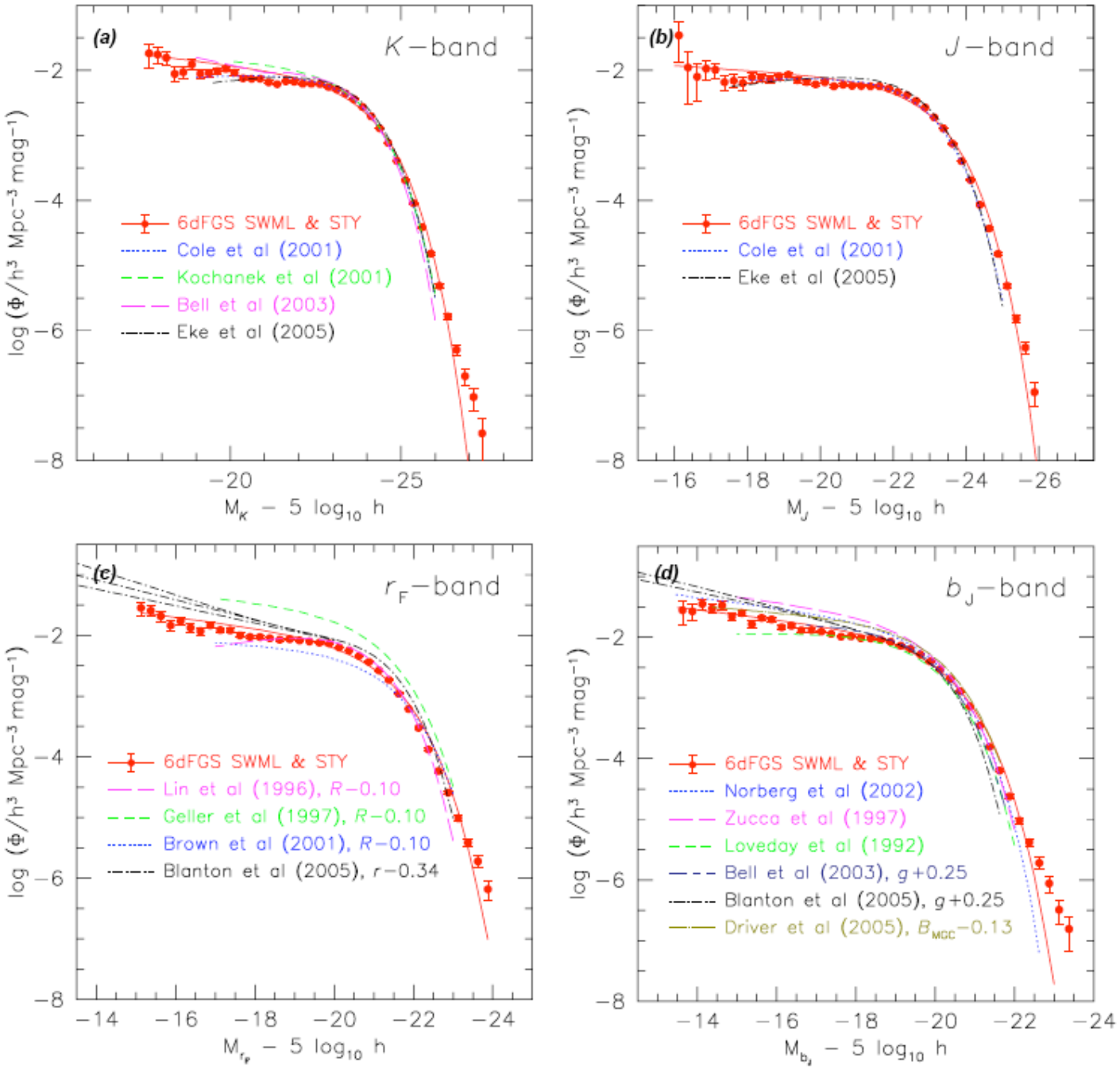
(a)
K−band
6dFGS SWML & STY
Cole et al (2001)
Kochanek et al (2001)
Bell et al (2003)
Eke et al (2005)
log (Φ/h³ Mpc⁻³ mag⁻¹)
M_K − 5 log10 h
(b)
J−band
6dFGS SWML & STY
Cole et al (2001)
Eke et al (2005)
M_J − 5 log10 h
(c)
r_F−band
6dFGS SWML & STY
Lin et al (1996), R−0.10
Geller et al (1997), R−0.10
Brown et al (2001), R−0.10
Blanton et al (2005), r−0.34
(d)
b_J−band
6dFGS SWML & STY
Norberg et al (2002)
Zucca et al (1997)
Loveday et al (1992)
Bell et al (2003), g+0.25
Blanton et al (2005), g+0.25
Driver et al (2005), B_MGC−0.13

Faint Galaxy Counts

1 point statistics !!!
Note:
(a) The galaxy luminosities evolve with redshift z (either passively, or because of a
higher star-formation rate at earlier times).
(b) The number density of galaxies can be higher at higher redshifts (for example due to later merging).

Given the luminosity function and counts one can learn about cosmology and/or discuss galaxy evolution …
Degeneracy can be partly broken if redshift distributions are made available.

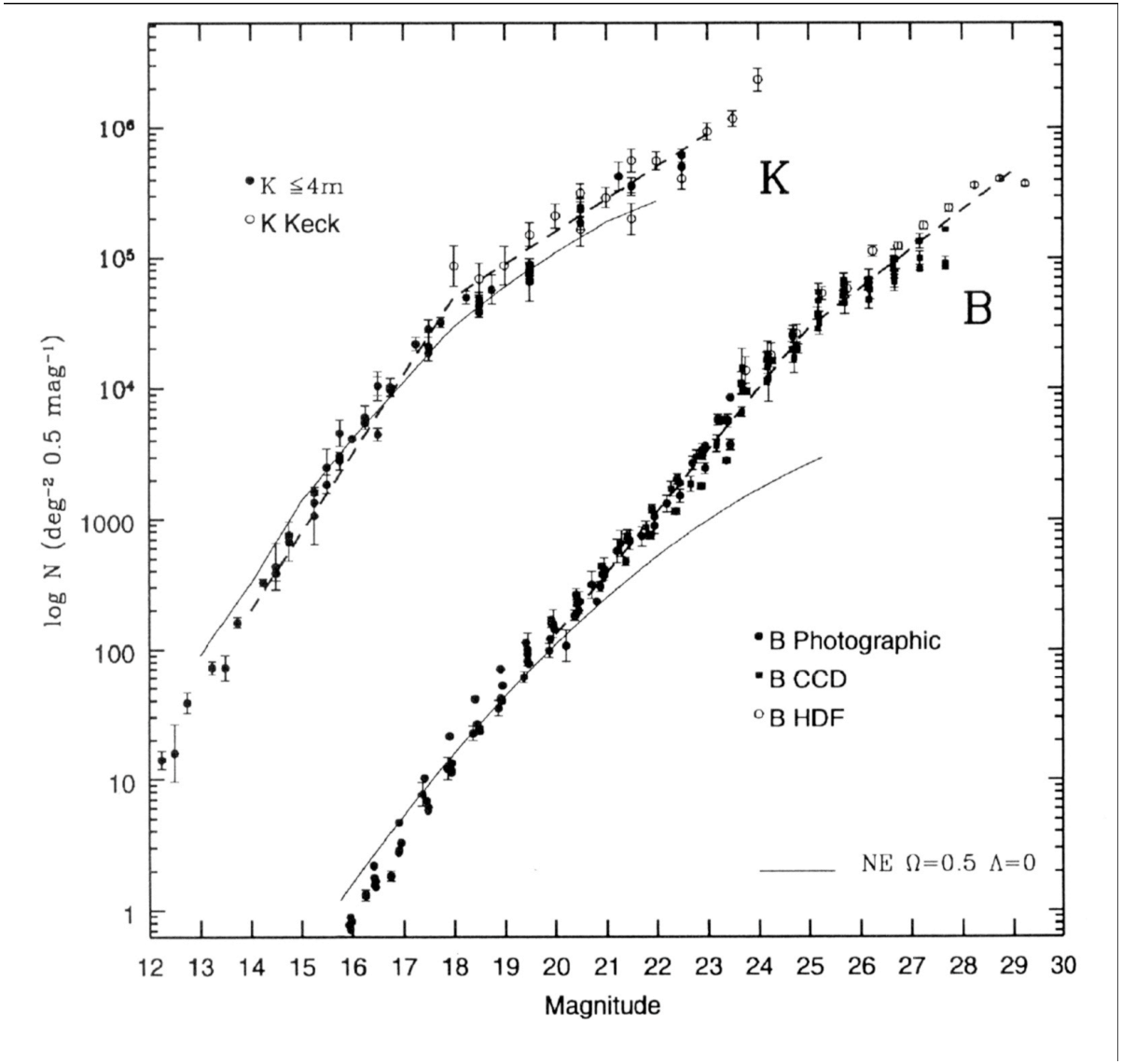
log N (deg⁻² 0.5 mag⁻¹)
Magnitude
K ≤4m
K Keck
K
B
B Photographic
B CCD
B HDF
NE Ω=0.5 Λ=0

The Tully-Fisher Relation

Relation between circular speed v_{circ} and luminosity of spiral galaxies:

$L \propto v_{circ}^{3\ldots4}$

(The power depends on the wavelength of L, because of changing M=L, star formation, etc.)

From the virial theorem, $v_{circ}^2 \propto M/r$

and the identity $L \propto \text{sigma } r^2$ (with Sigma: surface brightness) one obtains:

$L \propto (M/L)^{-2} \; v_{circ}^4 \; \text{Sigma}^{-1}$

Evidently the observed Tully-Fisher relation implies:

$(M/L)^{-2} \; \text{Sigma}^{-1} = \text{constant}$

Indeed, most bright spirals have similar mass-to-light ratios and surface brightnesses:

M/L = const and Sigma = const (the latter is called the "Freeman law").

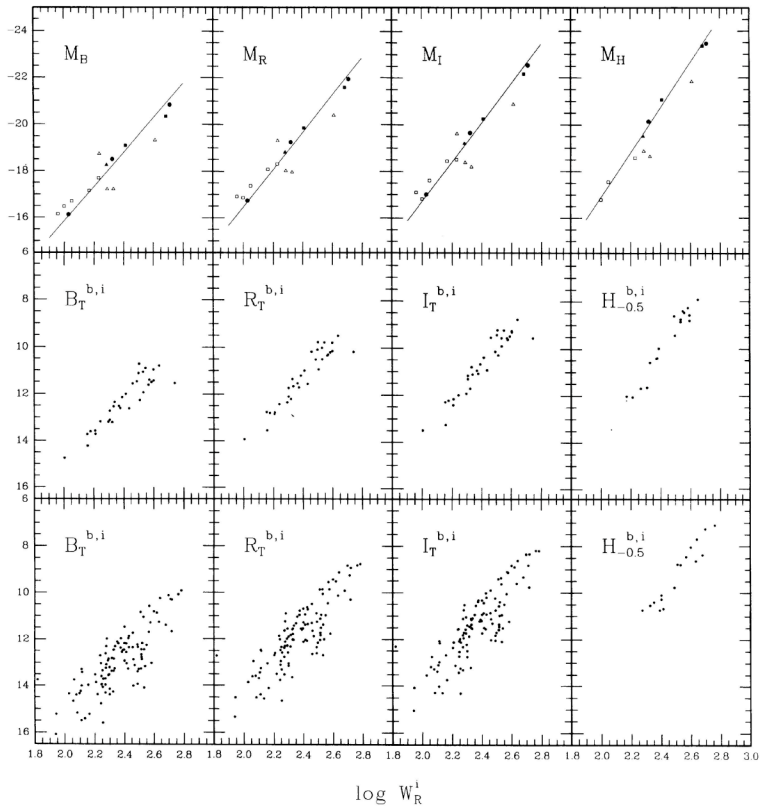

FIG. 11—*B*-, *R*-, *I*-, and *H*-band Tully–Fisher relations for the Local Calibrators (top), Ursa Major cluster members (middle), and Virgo cluster members (bottom). It is apparent from the figures that the slope of the relations increases going to longer wavelengths and the dispersion decreases. The variation in slope is thought to arise from the differing contributions to the observed bandpass made by greater fraction of young stars found in the lower-luminosity systems. The smaller dispersion at longer wavelengths is likely due to a reduction in the sensitivity to these effects, as well as those expected from extinction variations. Note the much larger dispersion found for the Virgo cluster data.

$W^i_R = 2v_{circ}$
v_{circ} can be deduced from HI observations;

correction for inclination adopting flattening of optical image.

see: Jacoby et al. (1992) PASP, 104, 599

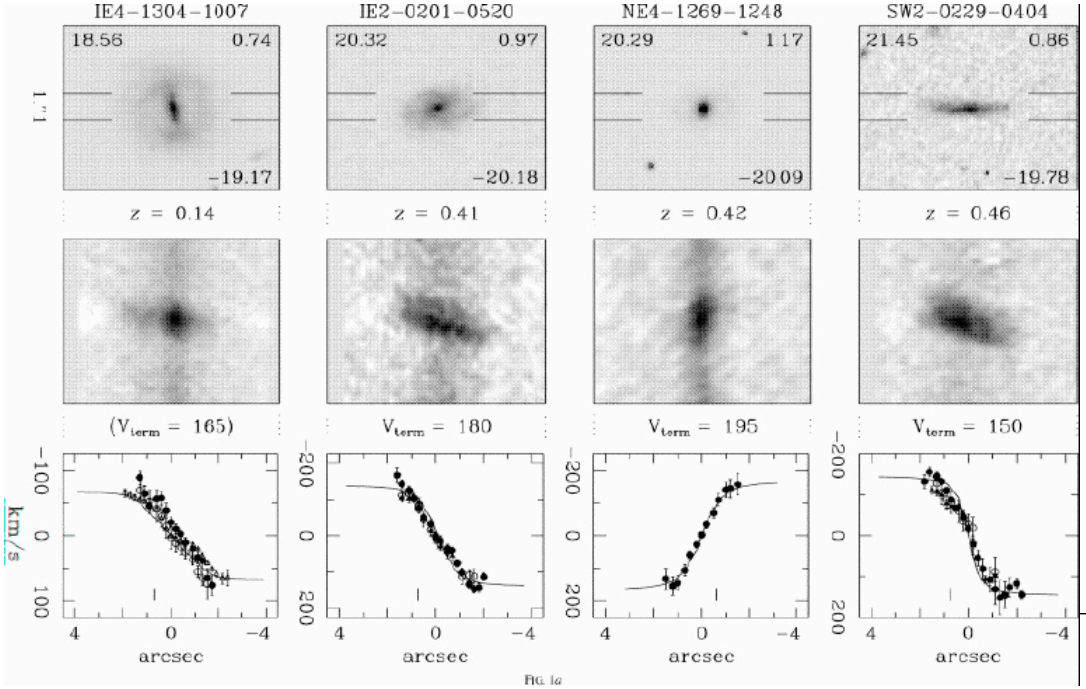

Tully–Fisher relation for spirals @ different z (Vogt et al., 1997, ApJ, 479, L121)

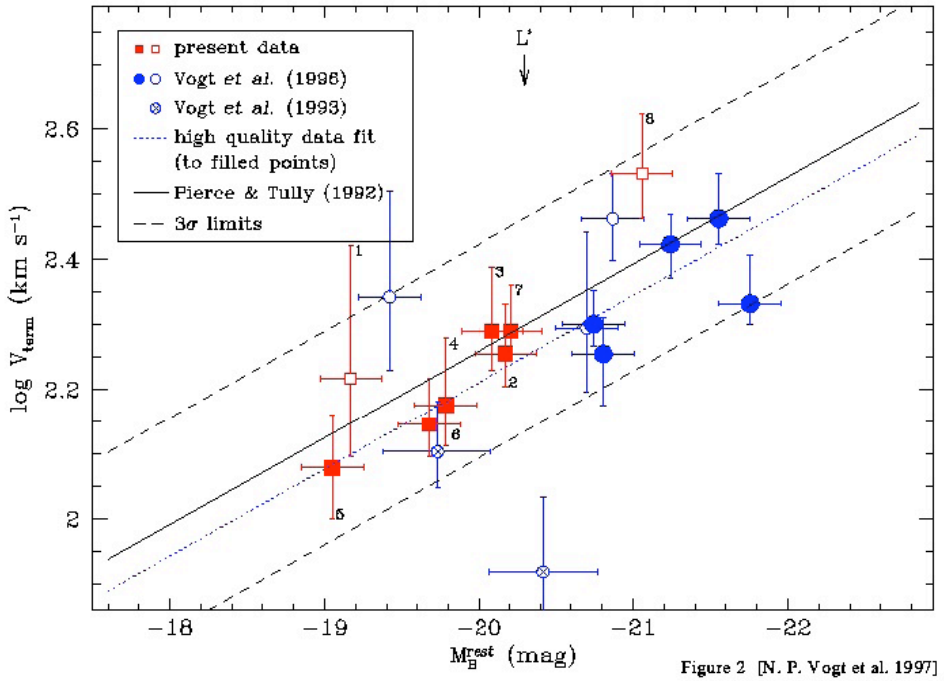

Figure 2 [N. P. Vogt et al. 1997]

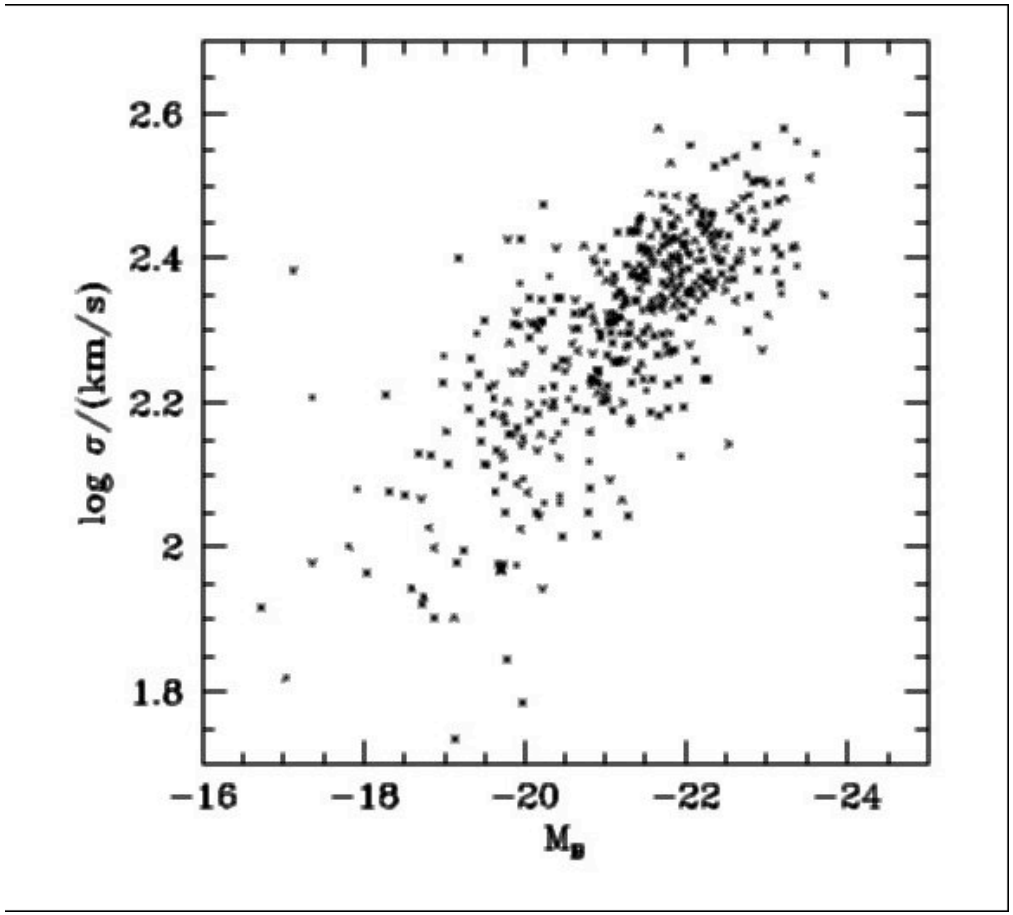

Faber-Jackson relation between central velocity dispersion and total magnitude of elliptical galaxies

L_B propto sigma ^{4}

Fundamental Plane of Elliptical Galaxies

A comprehensive set of global parameters of elliptical galaxies is:
The half light (or effective) radius r_e
The mean surface brightness $Sigma_e$ (or I_e) within r_e
The central velocity dispersion $sigma_0$
The luminosity L
The mass M of the visible matter

The following two relations relate these quantities:
$Sigma_e = L/2 / (pi\ r_e^2)$ (Definition of mean surface brightness)
$M/r_e = c\ sigma_0^2$ (Virial equilibrium)

with the structure parameter c which contains all unknown details about the galaxies' structure. Multiplication yields an expected relation for these parameters:

$r_e = c/(2\ pi)\ \ (M/L)^{-1}\ sigma_0^2\ Sigma_e^{-1}$

Because neither M=L nor c are expected to vary very much, the brackets are nearly constant and imply that ellipticals should define a plane-like distribution in the 3-space of their global parameters (r_e, $Sigma_e$, $sigma_0^2$).

Astonishingly, this plane is much better defined than naively expected, with very low dispersion perpendicular to the plane (implying a variance in the product of the brackets less than 10%) and a small but significant tilt (implying small but significant changes in the structure of ellipticals as a function of their luminosity or mass), see Djorgovski & Davis (1987), Dressler et al. (1987).

The observed so-called "fundamental plane" relation reads:

$r_e\ \ propto\ \ sigma_0^{1.4}\ Sigma_e^{-0.85}$

This is consistent with the theoretical expectation, if
(2 pi /c) (M / L) propto $M^{0.2}$ propto $L^{0.25}$
This implies a limitation of the variation of the dynamical structure ($sigma_0$), of the M/L of the stellar population, of the amount of dark matter within r_e, of the slope of the stellar initial mass function, and all other possibly varying parameters.
) Even though the kinematics of ellipticals can appear to be highly complicated in
detail, the objects must in fact be rather similar with respect to their global structureand their stellar M/L !

Note: The fundamental plane is an important distance indicator for elliptical galaxies, like the Tully-Fisher relation for spirals. At higher redshifts it is a useful indicator for the evolution of elliptical galaxies.

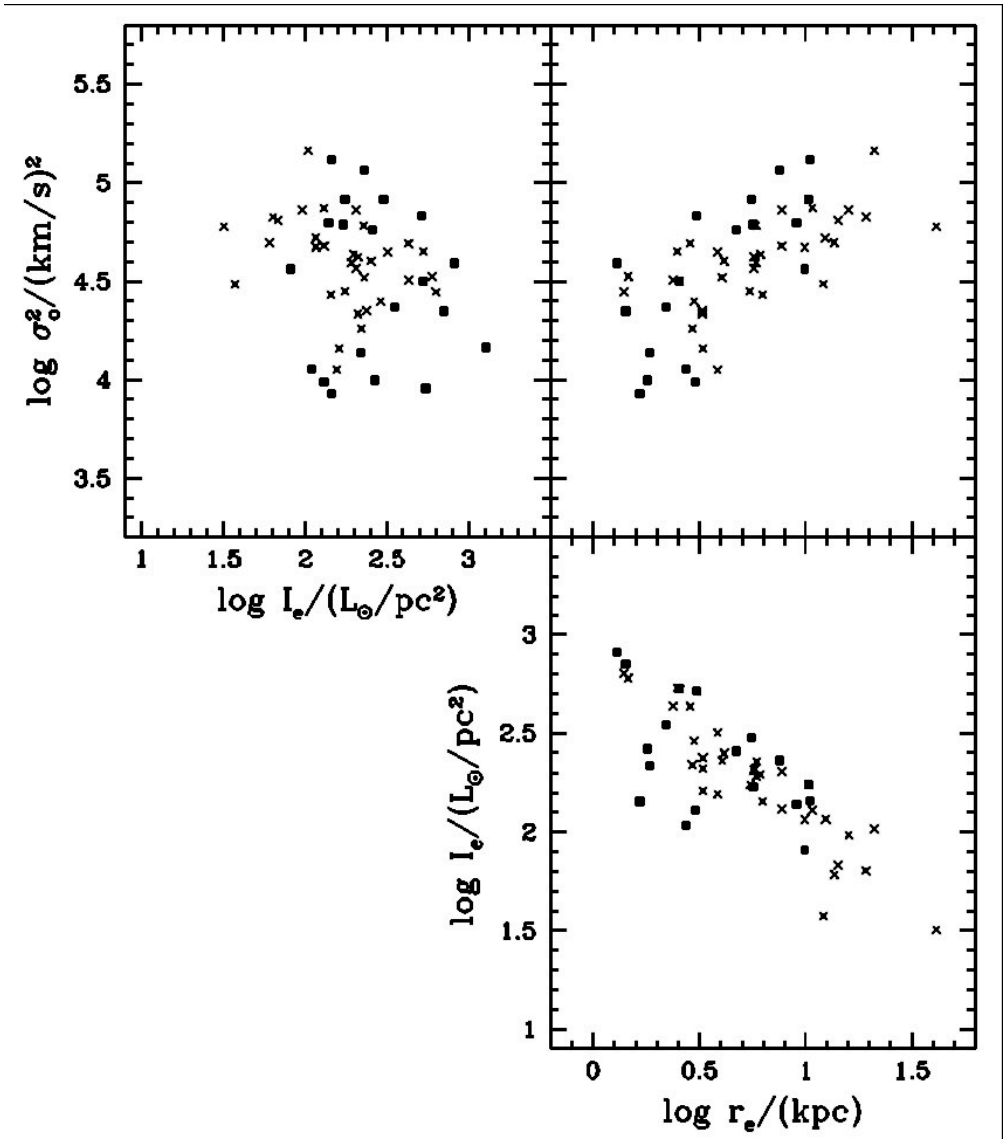
log $\sigma_o^2/(km/s)^2$
log $I_e/(L_\odot/pc^2)$
log $I_e/(L_\odot/pc^2)$
log $r_e/(kpc)$

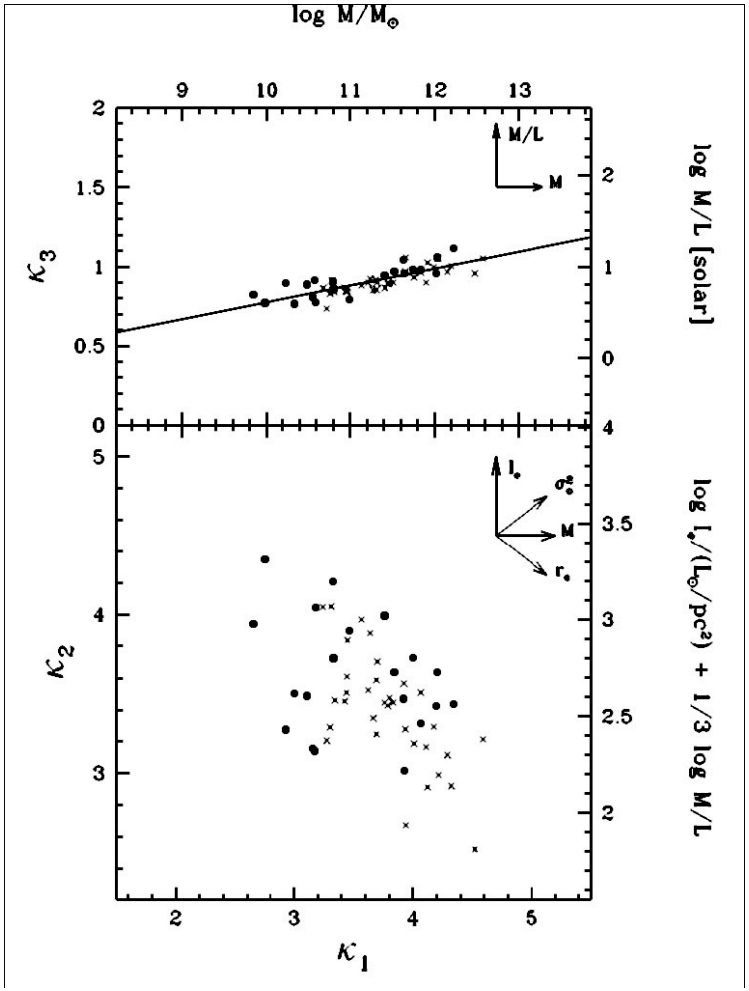
log $M/M_\odot$
κ_3
M/L
M
κ_2
I_e
σ_o^2
M
r_e
κ_1
log M/L [solar]
log $I_e/(L_\odot/pc^2)$ + 1/3 log M/L

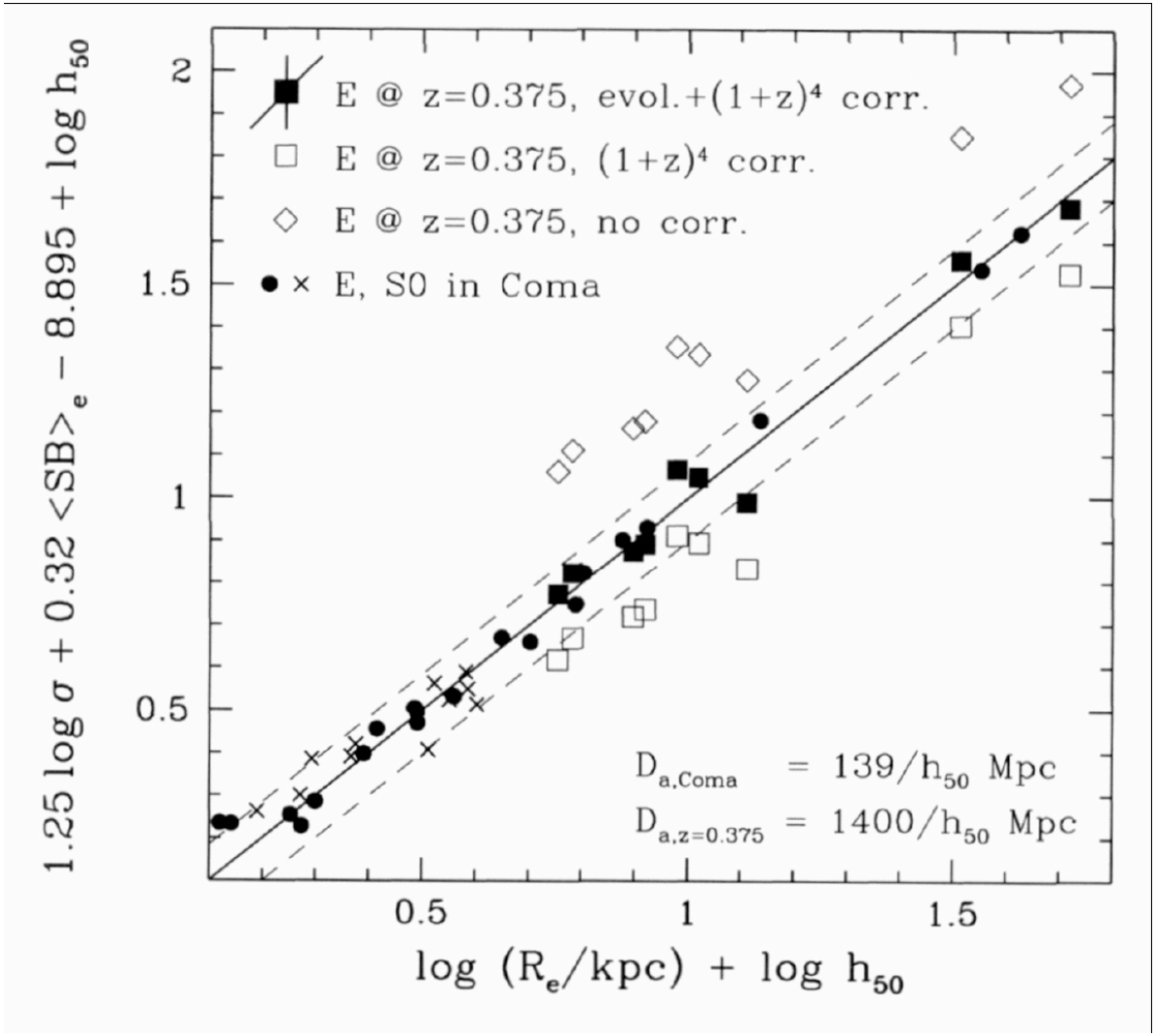

A comparison of physical effective radii of elliptical galaxies in the z = 0.375 galaxy cluster Abell 370 and the local Coma cluster.

Bender et al. 1998, ApJ, 493, 529

III - les galaxies « locales » vues par le SDSS

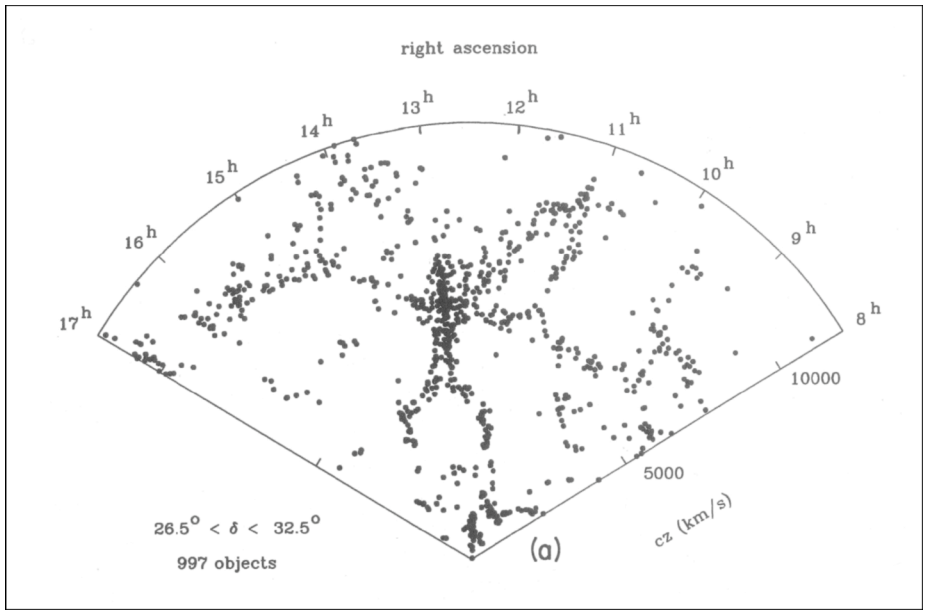

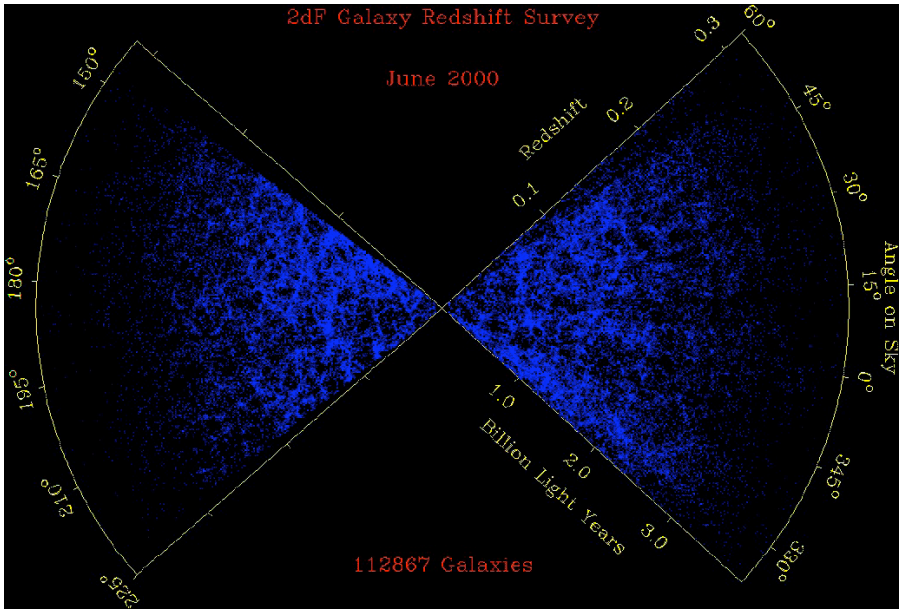

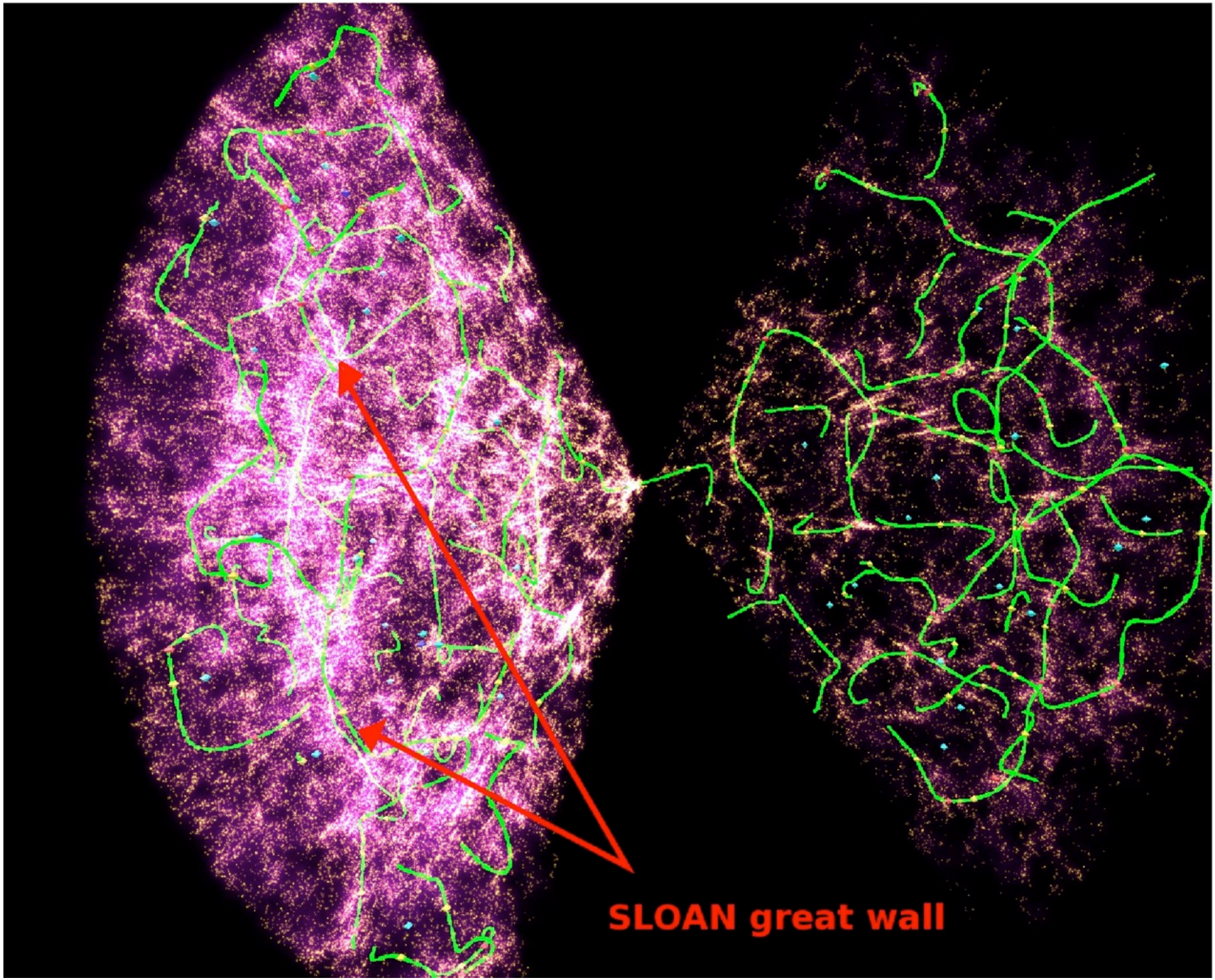
SLOAN great wall

The Vmax correction of the selection effects: the example of the size distribution of galaxies

As described in the last lecture, the sample is selected to be complete only to some magnitude, size and surface-brightness limits. In order to obtain the size distribution for the galaxy population as a whole, corrections must be made for these selection effects.
The Vmax method is widely used by SDSS people to do this.
The basic idea of the Vmax method is to give each galaxy a weight which is proportional to the inverse of the maximum volume (Vmax) within which galaxies identical to the one under consideration can be observed. For a given galaxy with magnitude r, Petrosian half-light radius R_{50}, surface-brightness μ_{50}, and redshift z, the selection criteria is used to define the value of Vmax in the following way:

1- The magnitude range $r_{min} \leq r \leq r_{max}$ corresponds to a maximum redshift $z_{max,m}$ and a minimum redshift $z_{min,m}$: $dL(z_{max,m}) = dL(z)10^{-0.2(r-rmax)}$; $dL(z_{min,m}) = dL(z)10^{-0.2(r-rmin)}$
where dL(z) is the luminosity distance at redshift z.
Note: K-correction and luminosity evolution effects are neglected in calculating $dL(z_{max,m})$ and $dL(z_{min,m})$. In general, the K-correction makes a given galaxy fainter in the observed r-band if it is put at higher redshift. The luminosity evolution has an opposite effect; it makes galaxies brighter at higher redshift. It turns out that including these two opposite effects (each is about one magnitude per unit redshift, see Blanton et al. 2002a; 2002c) has a negligible impact on the results.

2- The surface-brightness limit constrains the Vmax of a galaxy mainly through the dimming effect. The maximum redshift at which a galaxy of surface-brightness μ_{50} at z can still be observed with the limit surface-brightness $\mu_{lim} = 23.0$ mag arcsec^{-2} is given by
$z_{max,\mu} = (1 + z)x10^{(23.0-\mu 50)/10} - 1$

Note: K-correction and luminosity evolution are neglected again but also possible color gradients in individual galaxies.

3- The minimum size limit D_{min} (compact gals mistaken for stars or size measure way off due to PSF) also defines a maximum redshift $z_{max,R}$ given by
$dA(z_{max,R}) / dA(z) = R_{50} / 1.6''$ where dA is the angular-diameter distance.

The real maximum and minimum redshifts, z_{max} and z_{min}, for a given galaxy are therefore given by $z_{min} = \max(z_{min,m} , 0.005)$; $z_{max} = \min(z_{max,m} , z_{max,\mu} , z_{max,R})$ and the corresponding Vmax is
$V_{max} = 1 / 4\pi \int d\Omega\, f(\theta, \varphi) \int [z_{max}(\theta,\varphi) - z_{min}(\theta,\varphi)]\, dA(z)^2 / H(z)(1 + z)\, c\, dz$
where H(z) is the Hubble constant at redshift z, c is the speed of light, $f(\theta, \varphi)$ is the sampling fraction as a function of position on the sky, and Ω is the solid angle.

The apparent-magnitude limit only influences the number of galaxies at a given absolute-magnitude, and so it does not matter when we analyze the size distribution for galaxies with a given absolute magnitude. We can define a 'conditional' maximum volume,
$V^*_{max} = V_{max} / (4\pi)^{-1} \int d\Omega\, f(\theta, \varphi) \int [z_{max,m}(\theta,\varphi) - z_{min}(\theta,\varphi)]\, dA(z)^2\, H^{-1}(z)(1 + z)^{-1} c\, dz$
which takes values from 0 to 1, and gives the probability a galaxy with size R_{50} to be observed at the given absolute magnitude M. Given N galaxies in an absolute-magnitude (or mass) bin M ± dM, the intrinsic conditional size distribution f(R|M) can be estimated as:
$f(R|M) \propto \sum_{I=1\ldots N} (V^*_{max,i})^{-1}$ if $R - dR < R_i < R + dR$ where R_i and $V^*_{max,i}$ are the radius and the value of V^*_{max} for the ith galaxy.

NB: $M = m - DM(z) + 5 - K(z)$ where z is the redshift of the galaxy, DM(z) is the distance modulus (cosmology dependent) and K(z) is the K-correction.

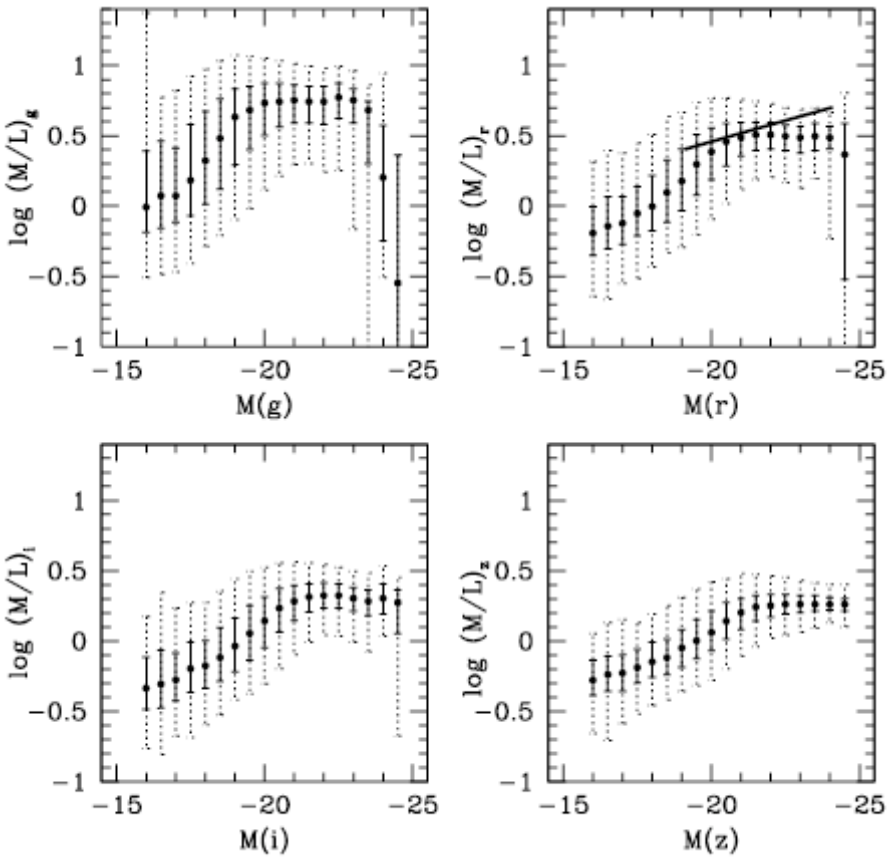

The total stellar mass of a galaxy divided by its observed luminosity (K-corrected to z=0.1) is plotted as a function of absolute magnitude in 4 SDSS bands. The solid symbols indicate the median mass-to-light ratio at a given magnitude, the solid errorbars indicate the 25th to 75th percentile ranges of the distribution and the dotted errorbars indicate the 5th-95th percentile ranges.
Mass-to-light ratios are plotted in solar units where $M_{\odot g}$ = 5.45, $M_{\odot r}$ = 4.76, $M_{\odot i}$ = 4.58 and $M_{\odot z}$ = 4.51 at z = 0.1. (Blanton et al 2002). The thick solid line is the mean relation between dynamical M/L (estimated from the stellar velocity dispersion) and r-band magnitude for a sample of early type galaxies from Bernardi et al (2002).

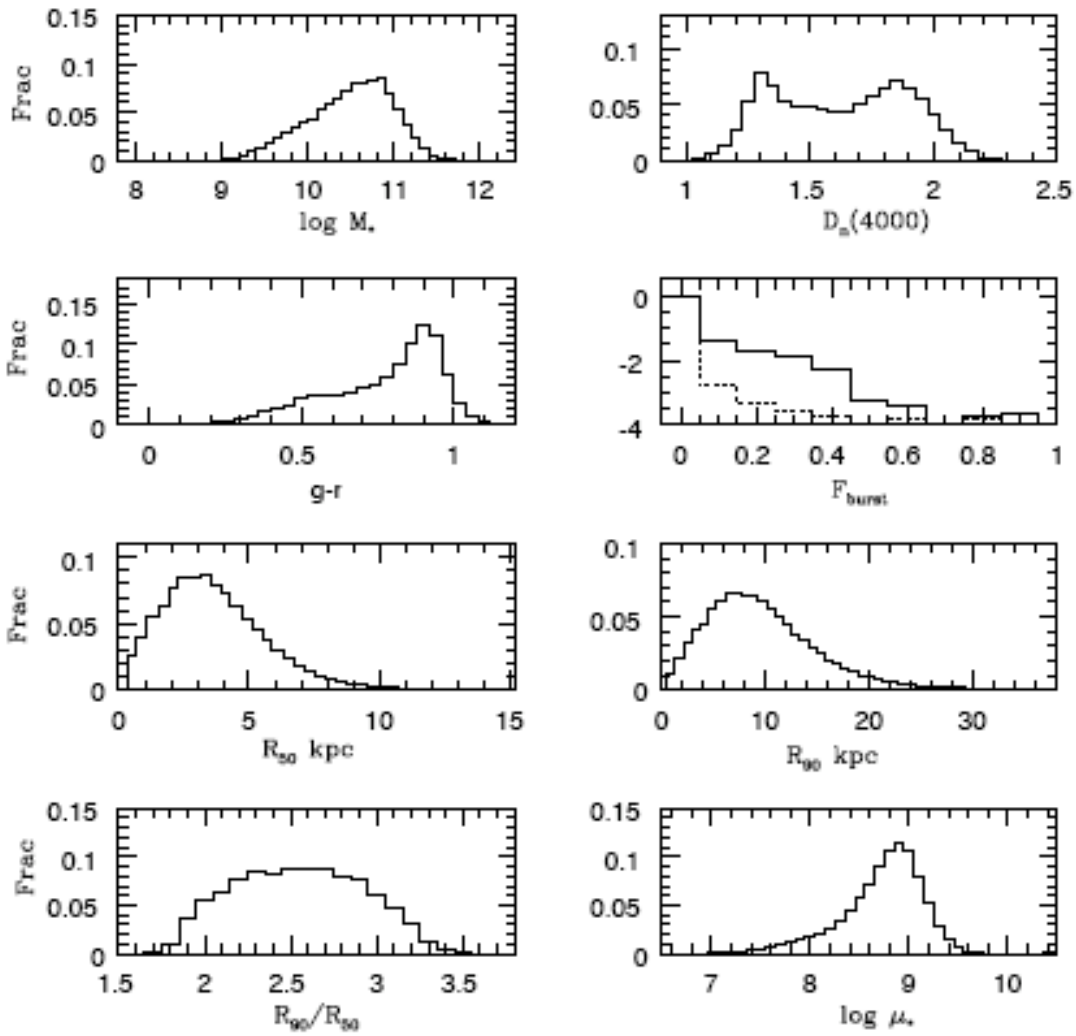

The fraction of the total stellar mass in the Universe contained in galaxies as a function of 1) log stellar mass, 2) Dn(4000), 3) g − r colour K-corrected to z=0.1, 4) F_{burst} (median) solid and F_{burst}(2.5%) dotted , 5) Petrosian half-light radius in the r-band, 6) Petrosian 90% radius on the r-band, 7) concentration index (R_{90}/R_{50}), 8) log surface mass density. The fraction is shown linearly in all plots except that for F_{burst} where the logarithm is given.

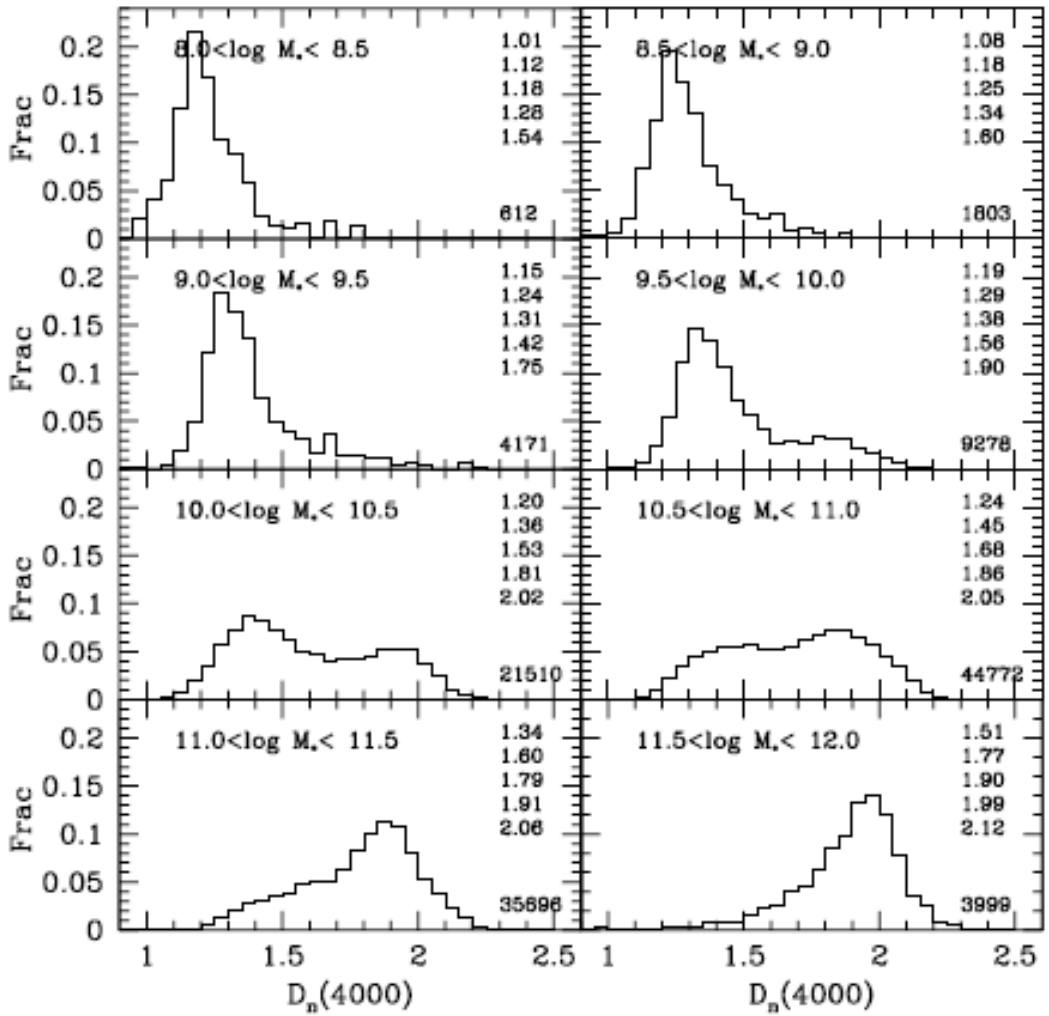

Histograms showing the fraction of galaxies as a function of Dn(4000) [4000 A break strength] in 8 different ranges of stellar mass. The numbers in the upper right corner of each panel list, from top to bottom, the 5th, 25th, 50th, 75th and 95th percentiles of the distribution. The number in the lower right corner is the number of galaxies contributing to the histogram.

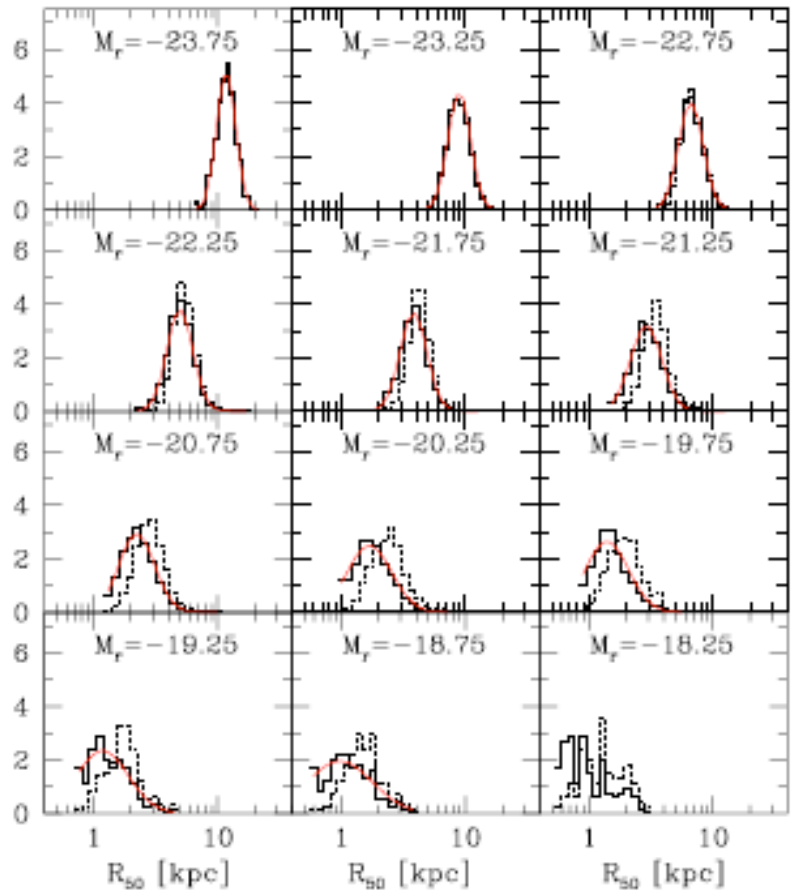

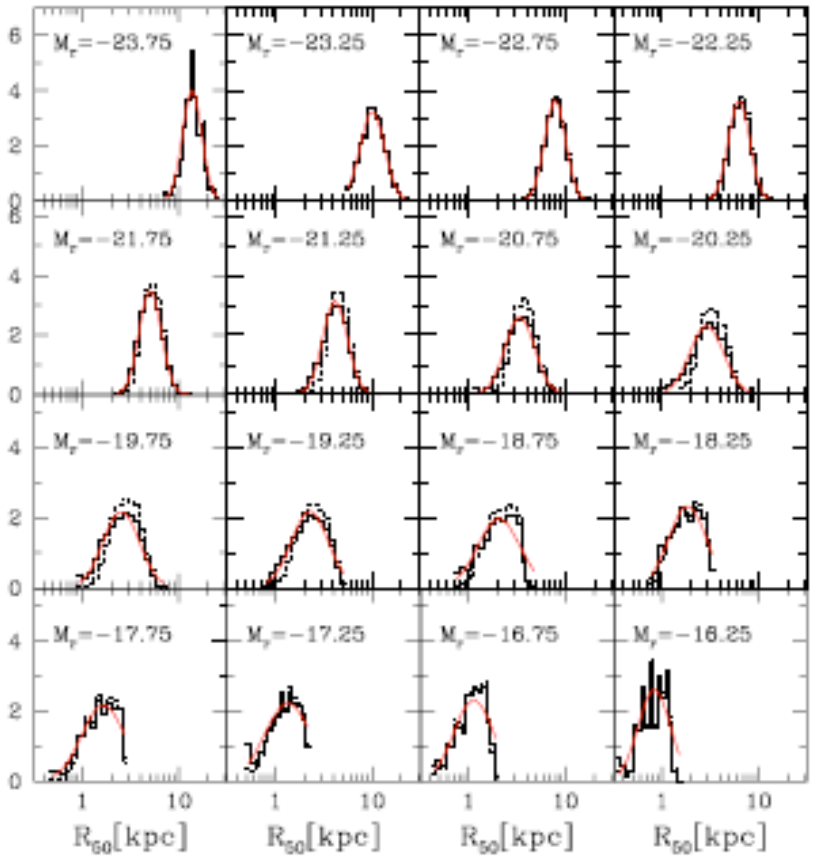

Histograms of Petrosian half-light radius R_{50} (in the r-band) for early-type (c > 2.86) and late type (c < 2.86) galaxies in different Petrosian r-band absolute-magnitude bins. The dotted histograms show the raw distribution, while the solid histograms show the results after a Vmax correction for selection effects. The solid curves are obtained by fitting the sizes to a log-normal distribution through the maximum-likelihood method.

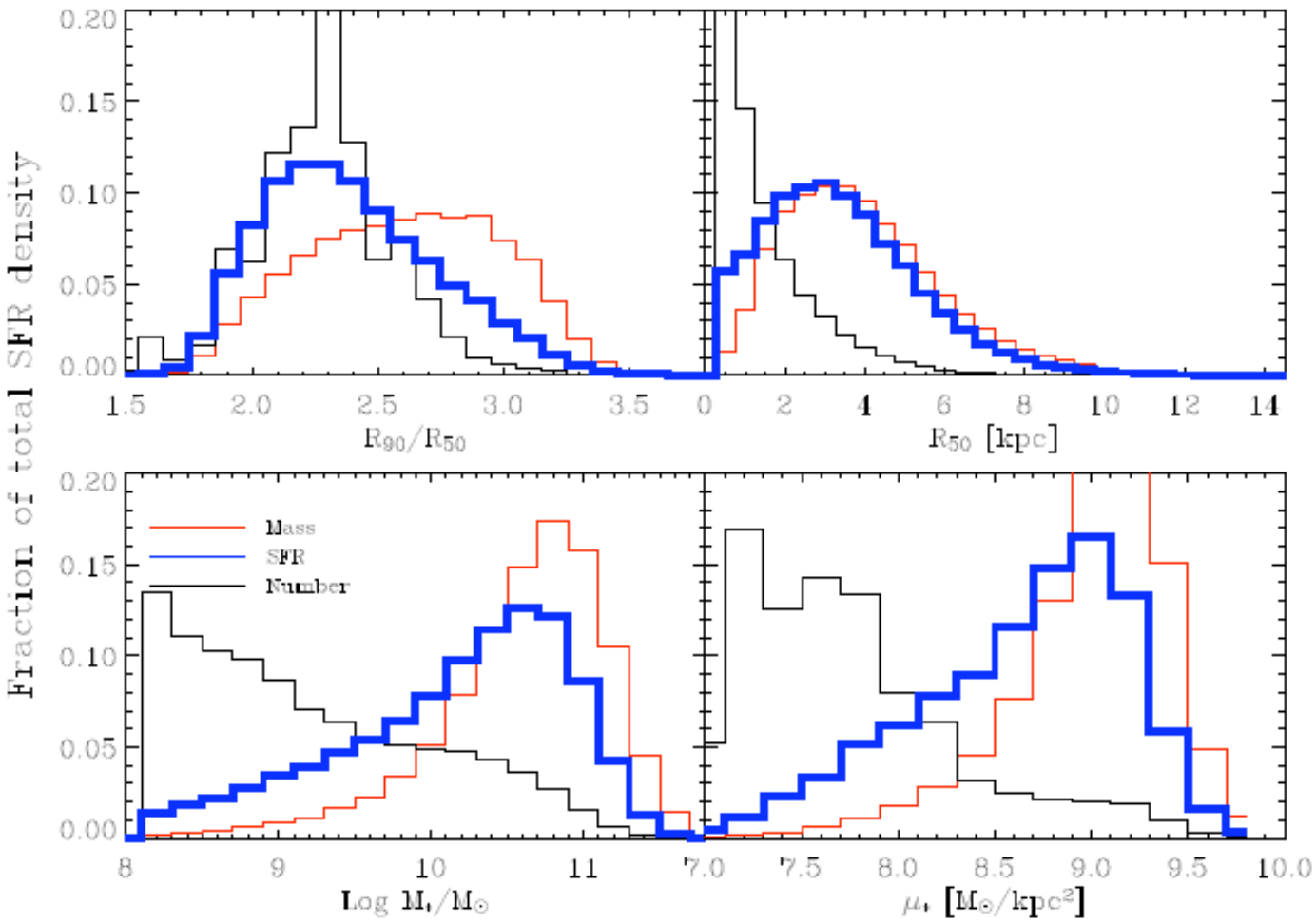

The contribution to the total number, mass and star formation density as a function of various galaxy parameters. The SF density is shown in blue, the mass density in red and the number density in black. Top left: The contribution to the different densities as a function of the concentration of the galaxies. Top right: The same, but as a function of the half-light radii of the galaxies. Lower left: The density contributions as a function of log stellar mass and Lower right: The contributions as a function of log of the stellar surface density in $M_{\odot}/kpc^2$

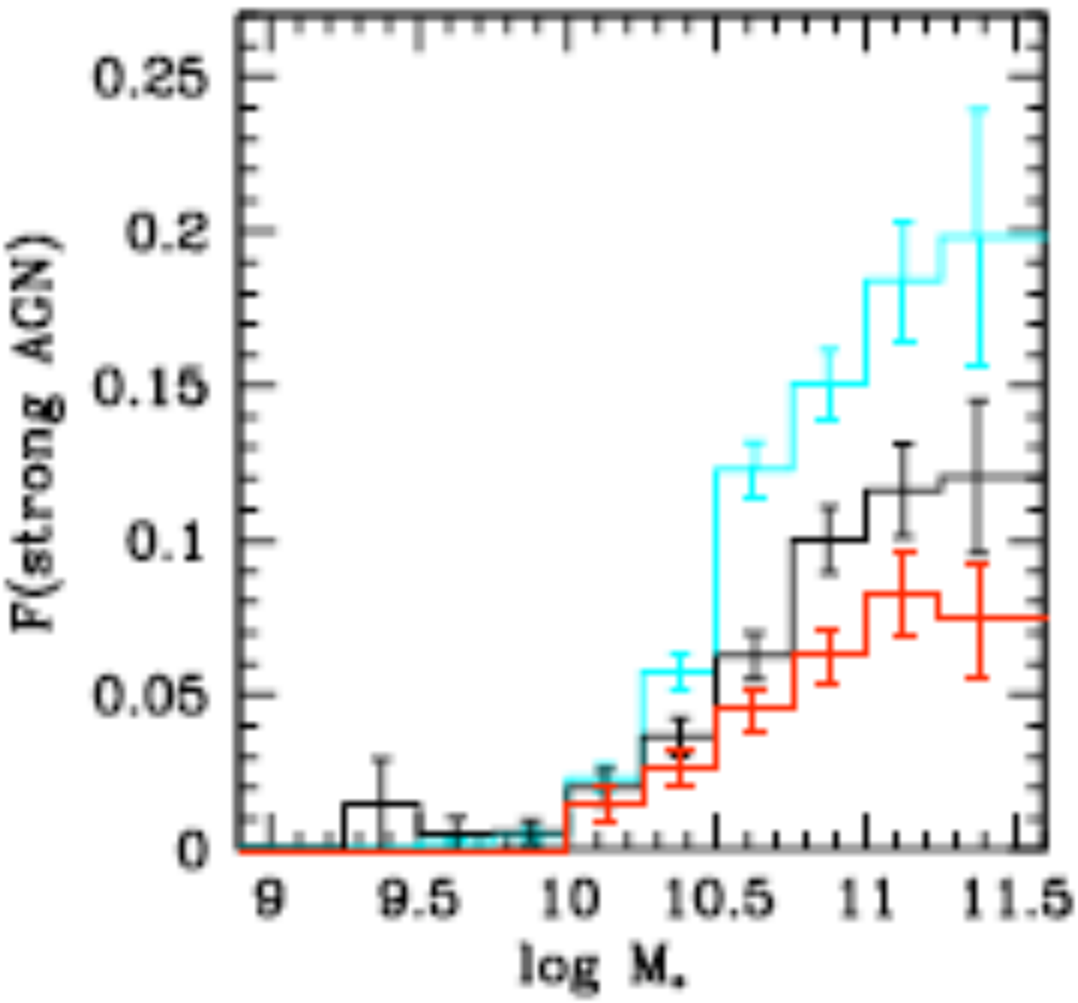

The fraction of galaxies containing AGN with L[OIII]> 10^7 $L_\odot$ is plotted as a function of stellar mass for three bins in density. Cyan is for galaxies with N_{neighb} = 0 – 1, black is for N_{neighb} = 7 – 11 and red is for N_{neighb} > 12

Mass-weighted stellar metallicity

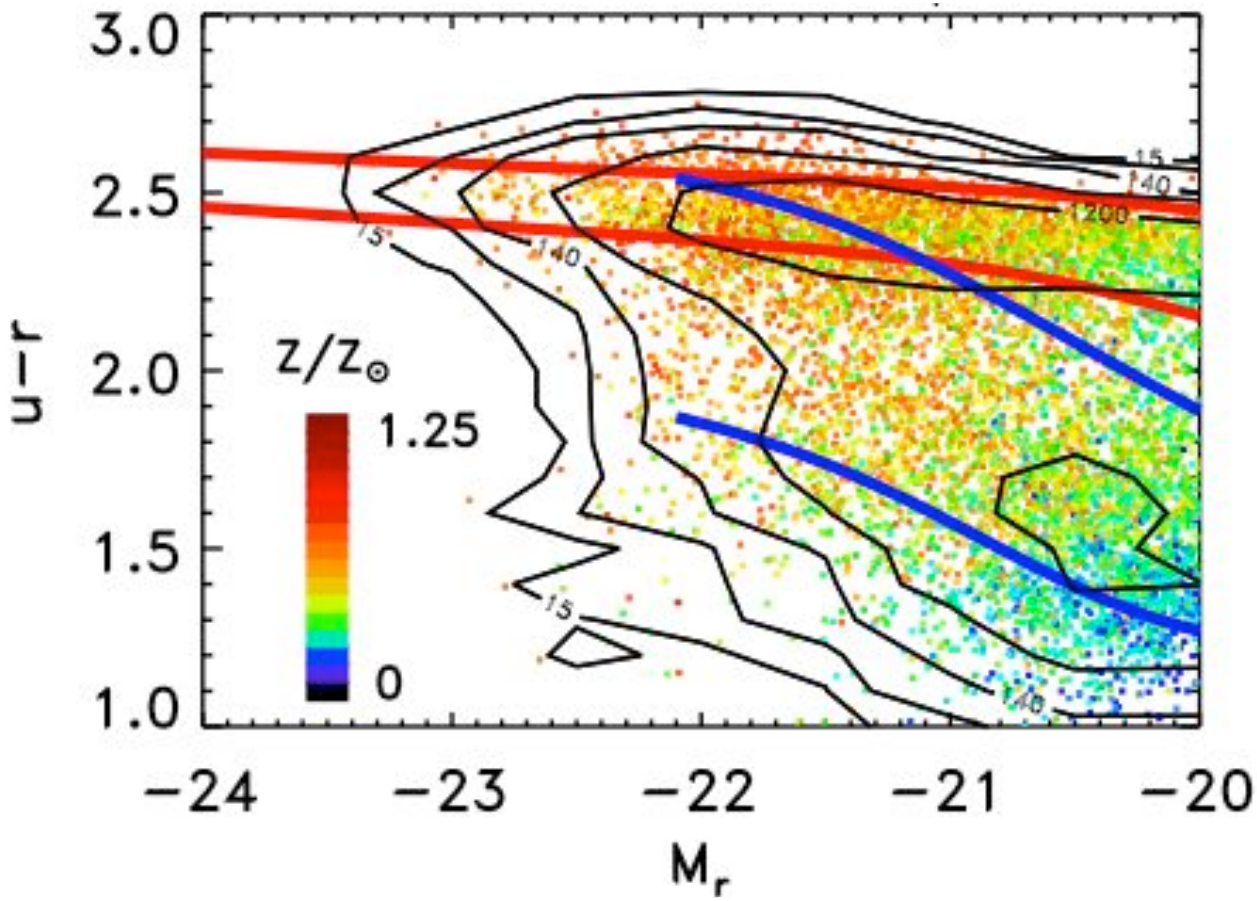

The red sequence colour-magnitude relation is a **metallicity effect** (more massive galaxies retain more metals)

Mass-weighted stellar age

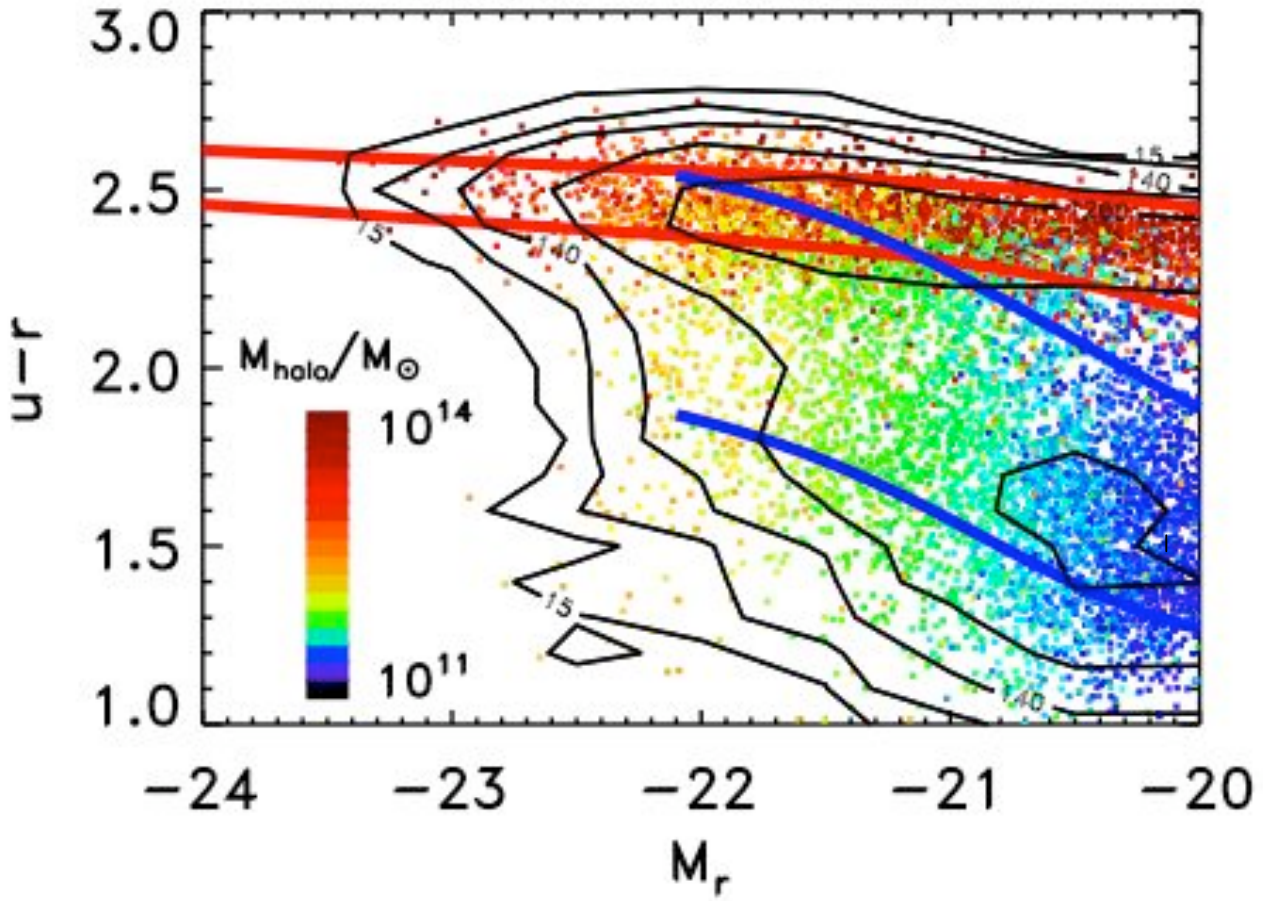

The colour difference between bright blue galaxies (Sa) and E/S0 is an **age effect** (the latter lack young stars)

Colour-morphology relation

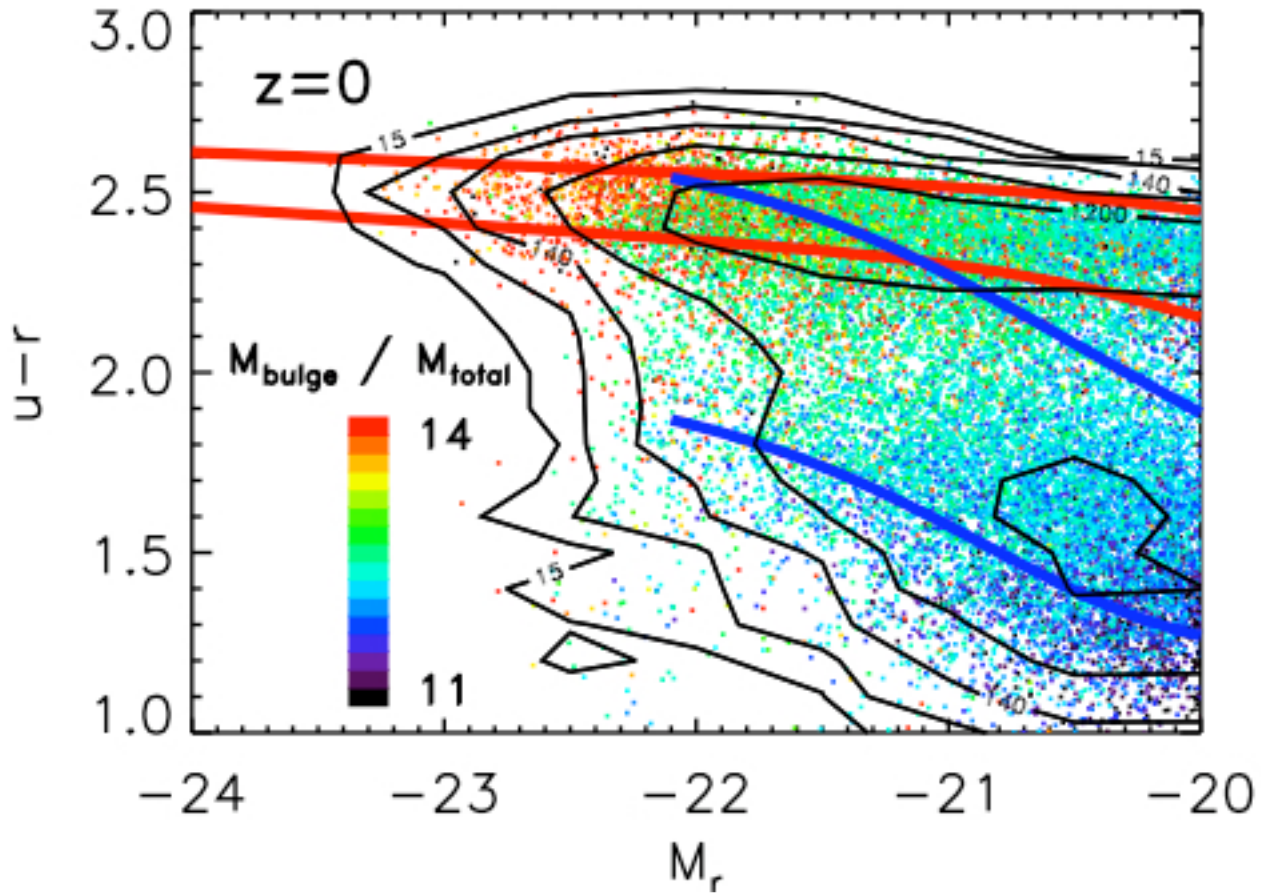

Colour - magnitude distribution

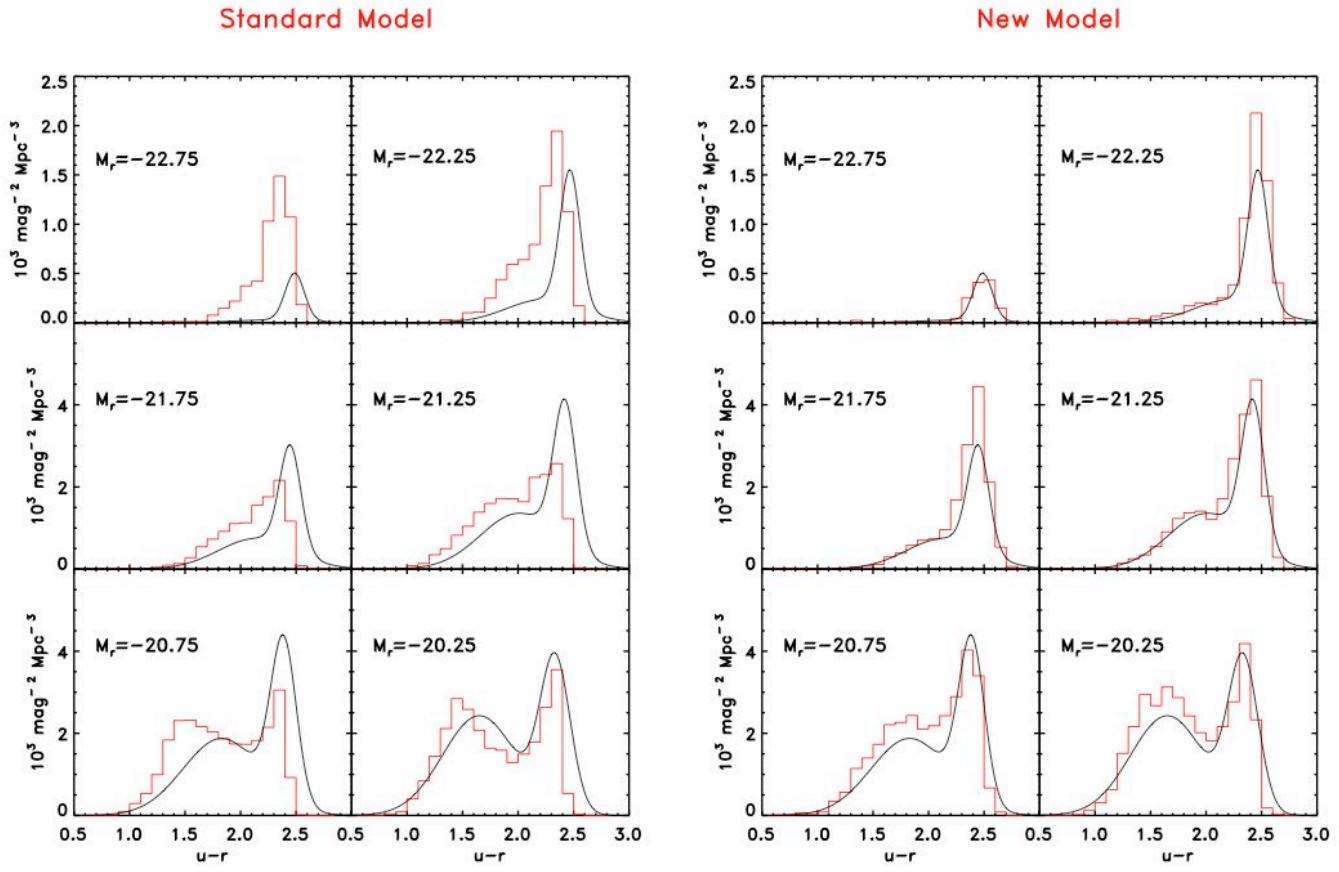

Cattaneo, Dekel, Devriendt, Guiderdoni and Blaizot 06

Galaxy Bimodality

LATE TYPE

Disk dominated

Blue, star-forming

Faint

Metal-poor

Field, small groups

EARLY TYPE

Bulge dominated

Red, passive

Bright

Metal-rich

X-ray groups, clusters

Black Holes in Spheroids

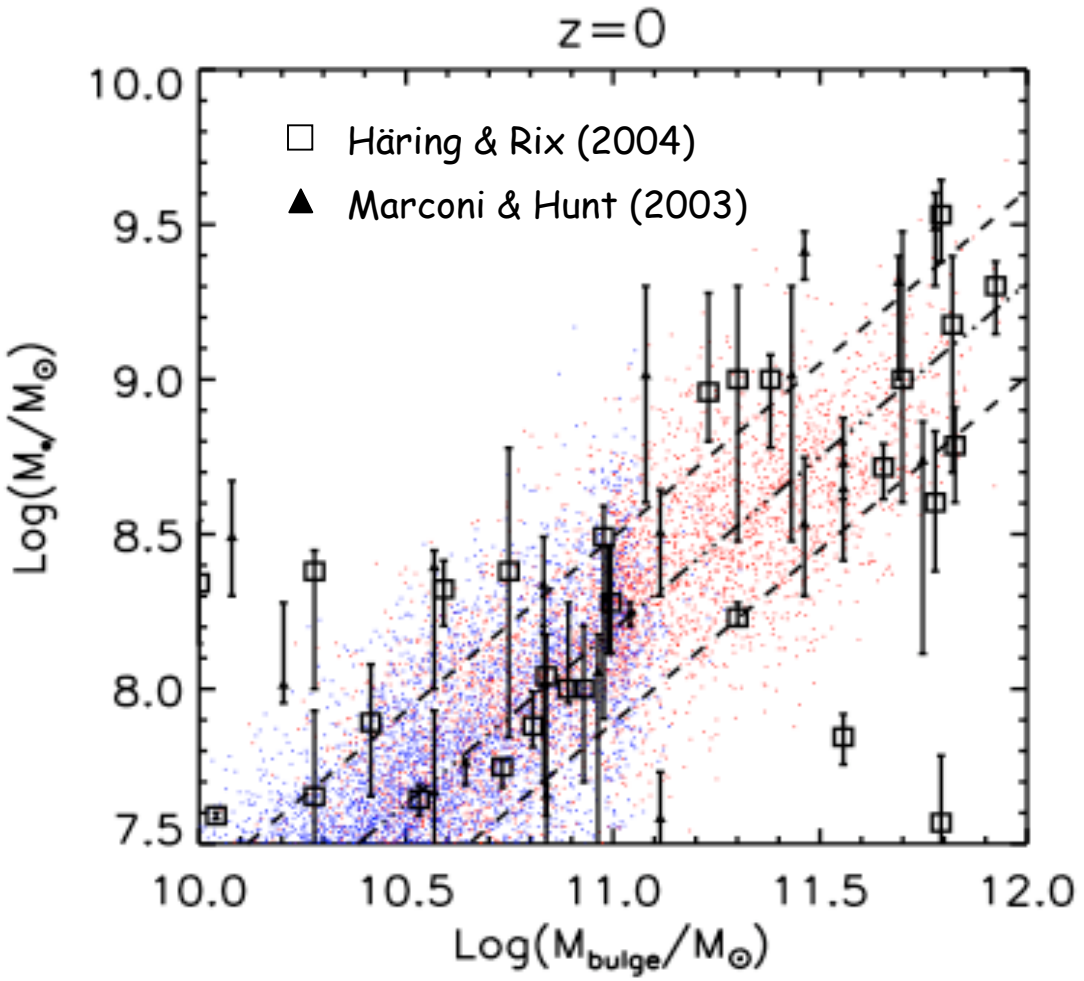

SDSS results (partial) summary

Downsizing

In massive objects, star formation starts and ends earlier

Bimodality

In most massive systems, shutdown of star formation/disc growth

Colour - morphology relation

Link gas accretion/star formation history - dynamical evolution

Black hole growth

Directly linked to the formation of the bulge component

IV- les galaxies a grand-z vues par la technique Lyman-break

HDF

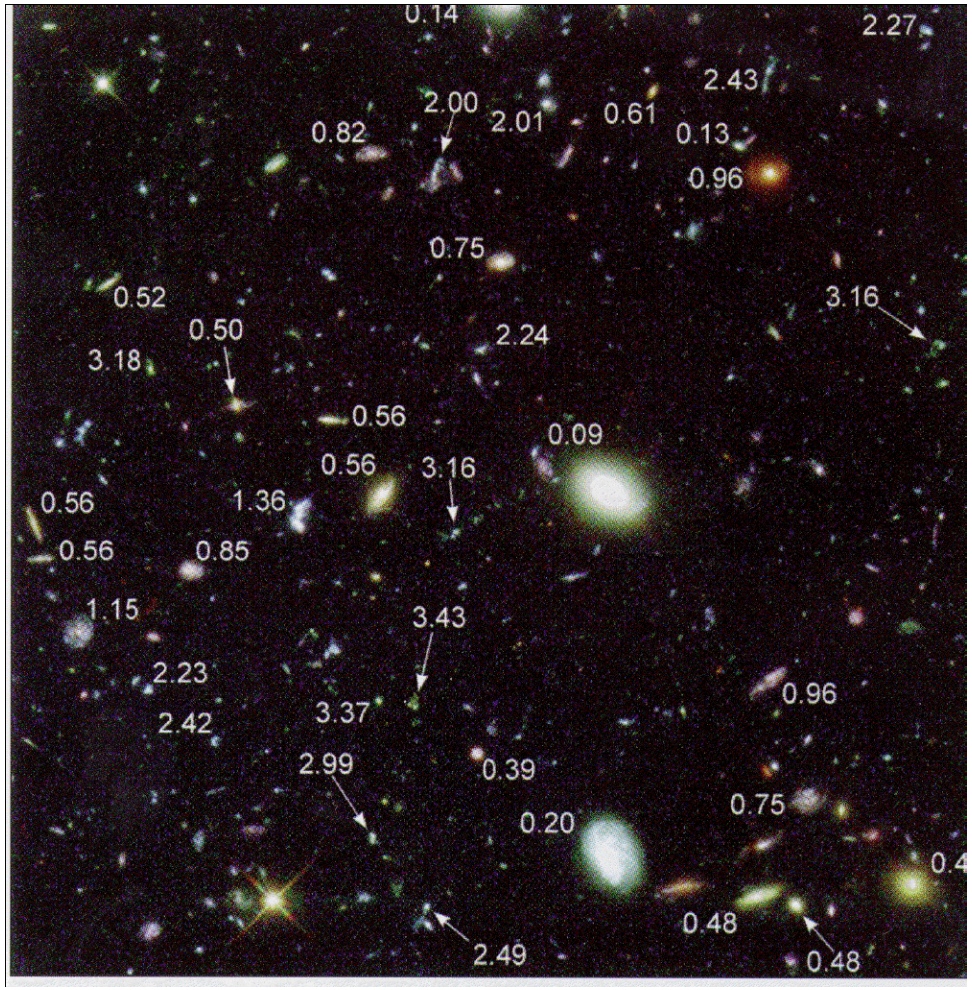

Problem:
For a long time high-redshift galaxies were too faint for spectroscopic observations. (This situation has changed as more and more 8-m and 10-m telescopes have become available.)
Solution:
Detection of the Lyman break by choosing appropriate filters (below the Lyman break practically all stars (and thus galaxies) do not emit much radiation).
Search concentrated on fields pointed at quasars with known redshift (hoping to
detect clusters of galaxies).
This method has lead to the detection of a number of galaxies at $z > 3$, the spectra of
which can now be obtained with the Keck, VLT, . . .
High-redshift galaxies generally show slightly increased star-formation rates.